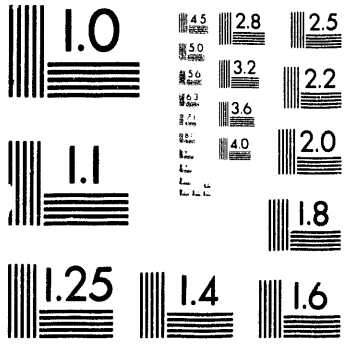
1.0
1.1
1.25
1.4
1.6
1.8
2.0
2.2
2.5
2.8
3.2
3.6
4.0
4.5
5.0
5.6
6.3
7.1

1 of 1

DOE/ER/40692-2

PROGRESS REPORT

U.S. DEPARTMENT OF ENERGY

Relativistic Heavy Ion Physics

DE-FG02-92ER40692

11/15/92-11/14/93

John C. Hill
Fred K. Wohn
Department of Physics and Astronomy
Iowa State University
Ames, IA 50011

DISCLAIMER

TABLE OF CONTENTS

ABSTRACT

In 1991 a proposal by the Iowa State University experimental nuclear physics group entitled "Relativistic Heavy Ion Physics" was funded by the U.S. Department of Energy, Office of Energy Research, for a three-year period beginning November 15, 1991. This is a progress report for the period May 1992 through April 1993.

In the first section, entitled "Purpose and Trends", we give some background on the recent trends in our research program and its evolution from an emphasis on nuclear structure physics to its present emphasis on relativistic heavy ion and RHIC physics. The next section, entitled "Physics Research Progress", is divided into four parts. First, we discuss our participation in the program to develop a large detector named PHENIX for the RHIC accelerator. Second, we discuss joining E864 at the AGS accelerator and our role in that experiment. Third, we outline progress made in the study of electromagnetic dissociation (ED). A highlight of this endeavor is an experiment carried out with the ^{197}Au beam from the AGS accelerator in April 1992. Fourth, we discuss progress in completion of our nuclear structure studies. In the final section a list of publications, invited talks and contributed talks is given.

PURPOSE AND TRENDS

The primary emphasis of the Iowa State University experimental nuclear physics program is the study of nuclear matter under extreme conditions of temperature and density by means of relativistic heavy ion collisions. This new emphasis began in July 1990 when we joined a collaboration to build a di-muon detector for the RHIC accelerator at Brookhaven. Later, as detector planning evolved, we joined together with others to build a large detector named PHENIX for RHIC. PHENIX will emphasize the study of photons and di-leptons produced in relativistic heavy ion collisions with a major motivation being to produce and detect signals from the quark-gluon plasma (QGP).

The major effort of our group will be to design and implement the first-level trigger for PHENIX in collaboration with the Engineering Services Group of the USDOE Ames Laboratory. That group has extensive relevant experience since they designed the data acquisition system for the Hadron Projection Chamber on the DELPHI detector at the LEP collider at CERN. We also have participated in the RD 10/45 R&D experiment at the AGS accelerator whose purpose is to measure the transport properties of hadrons and muons in various absorbers. We also will be involved in the R&D program at the AGS test beam in Summer 1993.

A second aspect of our program involves the search for strange matter and antinuclei with the 11 GeV/nucleon Au beam from the AGS accelerator. This is a new initiative on our part and also provides us with the opportunity to be involved in a large scale relativistic heavy ion experiment and "do some physics" before RHIC comes on line near the end of the decade. In March 1993 we were invited to join the E864 collaboration to participate in an experiment entitled "Measurements of Rare Composite Objects and High Sensitivity Searches for Novel Forms of Matter Produced in High Energy Heavy Ion Collisions". This experiment is scheduled to start running at the AGS in 1994. Our role in the experiment is to design and build the late-energy trigger which must be operational for taking data in 1995.

A third aspect of our program is the study of electromagnetic dissociation (ED). ED is a process in relativistic heavy ion reactions in which intense electromagnetic fields excite the nucleus through the exchange of virtual photons. ED is predicted to strongly dominate ultrarelativistic heavy ion reactions with heavy projectiles (due to the very intense electromagnetic pulse produced by ultrarelativistic heavy ions), thus it has important implications for the design of experiments and the next generation of heavy ion colliders. A proposal, AGS experiment E862, by our group to extend our ED studies using the 11 GeV/nucleon ^{197}Au beam from the AGS-booster accelerator, was approved in June 1990 and initial running was carried our at the AGS in April 1992. In April 1993 a proposal by us to measure ED at the CERN-SPS was approved as experiment NA53 and will run in 1995 using the 160 GeV/nucleon ^{208}Pb beam.

In view of our new commitment to relativistic heavy ion physics with future experiments at RHIC as the centerpiece of our program, we are phasing out our efforts in nuclear structure physics. Our final effort in that regard is toward completion of the dissertation of Mr. Vo by the end of 1993.

In this report we outline progress made from May 1992 through April 1993. The grant covers the three-year period from November 15, 1991 to November 14, 1994. Progress expected in the next year and our plans for the future are outlined in a proposal for funding of the third year (November 15, 1993 to November 14, 1994) of our three-year grant.

PHYSICS RESEARCH PROGRESS

A. Participation in RHIC Detector Development

The participation of the Iowa State experimental nuclear physics group with RHIC began in July 1990 when we joined the collaboration to build a di-muon detector. Along with many of our colleagues from the di-muon collaboration, we subsequently joined the larger collaboration to design and build the PHENIX detector which will emphasize the study of di-leptons and photons.

We also joined the PHOBOS detector collaboration, but in view of our major responsibilities in the PHENIX project, we withdrew from PHOBOS in February 1993. The Iowa State group has the major responsibility for designing and implementing the first-level trigger for the PHENIX detector. The concept for such a role began in October 1990 when Glenn Young (ORNL) visited Ames to join us in discussions with Harold Skank and Bill Thomas of the Ames Laboratory Engineering Services Group (ESG). The ESG is uniquely suited to work on electronics for PHENIX due to their experience in developing the data acquisition system for the hadron projection chamber (HPC) for the DELPHI detector at the LEP collider at CERN. In April 1992 Glenn Young and Leo Paffrath (BNL) visited Ames for two days to discuss the role of our group in electronics and triggering for PHENIX. In March 1993 we hosted at Ames a meeting of the PHENIX Online group for discussions of trigger and data acquisition issues.

The Iowa State group joined the RD-45 experiment which was funded through R&D funds for RHIC. The goal of this experiment was to measure leakage of hadrons through a series of filters upstream from a muon detector. The experiments were carried out using test beams from the AGS accelerator of particles (p,π,μ,e) in the momentum range from 1 to 10 GeV/c. Hill, Wohn, and our graduate student Ewell participated in both the preparations for and running of the RD-45 experiment in Summer 1992.

2. Progress in the PHENIX Level-1 Trigger Design

The major contribution to the PHENIX detector effort by the Iowa State Group will be the level-1 trigger. We have formed the Ames Trigger Group, which consists at present of 4 physicists (2 Principal Investigators, 1 postdoc, and 1 grad student) and 4 electronics engineers (3 Ames Lab staff and 1 grad student). The Ames Trigger Group will cover all aspects of the Level-1 Trigger for PHENIX - design, prototype testing, production, assembly and final testing at RHIC. Our group, the level-2 trigger group, and the data acquisition group are the three major components of the PHENIX Collaboration's Online Group, which is headed by Glenn Young (ORNL).

The level-1 trigger is crucial to the experimental program at PHENIX. Only events that pass one (or more) of the various level-1 triggers will be retained for further analysis by

the level-2 trigger. Therefore the level-1 trigger philosophy is to accept as many events as possible that can be classified as candidates for interesting physics. Rejection of some of the level-1 candidates by the level-2 trigger (or by higher levels) can be done on the basis on tighter restrictions and/or different algorithms than those used at level 1. However, the level-1 trigger must be able to control the rate of accepted events in order to allow the entire system, from level 1 until the final output to data tapes, to digest the incoming data stream without suffering deadtime losses. This is accomplished for the PHENIX detector by selecting a pipeline architecture. The level-1 trigger follows a "clock-based" pipeline, where each clock tick is the 112-ns beam crossing rate. The depth of the level-1 pipeline will be 32 ticks, or 3.58 μs. Subsequently, the level-2 trigger follows an "event-based" pipeline, where only events accepted at level 1 are allowed to enter the event pipeline.

Six of the detectors that make up the PHENIX detector will be used in the level-1 trigger. The six detectors are Beam-Beam, Silicon MVD (Multiplicity Vertex Detector), RICH (Ring Imaging Cherenkov), TOF (Time of Flight), EMCal (Electromagnetic Calorimeter) and Muon ID (Identifier) detectors. None of the tracking detectors (drift and pad chambers) will be used at level 1 because of the inherently slow speed of such detectors. For charged particles, this means that no momentum information can be used at level 1, since determining momenta requires tracking information. However, the main objective of the level-1 trigger is to identify the events that have candidates of interest, and for this tracking is not necessary. The phrase "candidates of interest" means the combinations of particles for physics of interest, thus combinations such as electron pairs, muon pairs, hadrons, and photons. The level-1 trigger will use the TOF trigger to select hadron candidates, with additional information from the Beam-Beam detector about whether there is a valid start time (from Beam-Beam) to permit an accurate time-of-flight measurement using the TOF stop time. Photon candidates will be identified by the EMCal, and muon candidates by the Muon ID. Both the RICH and the EMCal will be used to identify electron candidates.

Since the most interesting events are central-collisions that have high multiplicity, the level-1 trigger will generate multiplicity information from both the Silicon MVD and the EMCal. A sum over the MVD of charged particle hits will give one, and the other will be a sum, over the four EMCAL walls, of the total energy (which, due to the rapidity covered by the EMCal is mainly the transverse energy E_t). They give two alternatives for determining the "centrality" of a collision.

Control of the data rate will be accomplished in the level-1 trigger by using, in conjunction with the combinations of particle candidates, different prescale factors for different multiplicity ranges. To pick a simple example, there will be a trigger called Photon-1 that accepts single photons above a relatively high energy threshold, such as 2-3 GeV. That is, if any one of the 7000 EMCal trigger units (4x4 arrays of PMT towers) were to have an energy above the threshold, then that event would be kept, provided it would also pass the prescale requirement. With binary prescale factors 2^N, only 1 of each 2^N events passes the prescale requirement. Thus, to select every photon means the factor N must be 0. However, if this were to be done for the Photon-1 trigger, the rate of accepted events would be too high

without imposing multiplicity prescaling.

By using prescale factors on "global" parameters such as multiplicity, we expect to be able to "flatten out" the number of events accepted for the selected multiplicity ranges. Our plan for using prescalers for each of the level-1 triggers permits us to obtain "sampling mode" data of various types. This means that the number of triggers will be in the range of 100-200, in order to permit several values of multiplicity-prescale combinations for each of the particle combinations of interest. Normalization-type triggers with less restrictions would be included, but with high prescale factors. (For example, "Min Bias" events could be kept at a very large prescale factor such as 2^{20}.)

In addition to the obvious particle candidate types, such as 2 (or more) electrons in the RICH or 2 (or more) muons in the Muon ID, there are some less obvious types that must also be included in the level-1 triggers. One is the electron-muon combination that is needed in order to determine the substantial contributions from "open charm" decays to the observed dilepton channels (e^+e^- and $\mu^+\mu^-$). It is worth noting here that, due to combinatorics (such as an electron from each of 2 different decays) we need to accept all 2-electron combinations (e^+e^+ and e^-e^- as well as e^+e^- and e^-e^+). This is implicit in all level-1 triggers since there is no selection at level 1 on a particle's charge.

Chapter 11 of the PHENIX CDR (Conceptual Design Report) provides a detailed discussion of the various level-1 triggers we have designed. The level-1 trigger discussion comprises CDR pages 11-41 to 11-66 and is provided in the Appendix to this report. The initial cost estimate for the level-1 trigger was done by us in conjunction with PHENIX management, in particular with Leo Paffrath (Project Engineer) and Glenn Young (Deputy Project Director). A total construction cost for the level-1 trigger of $1.2M was estimated.

3. Progress with PHENIX Detector Simulations

Dr. Athan Petridis was hired in July 1992 to initiate at ISU an involvement with the PHENIX detector simulations. Since our involvement as a trigger group would be with the entire detector, Dr. Petridis' first task was to develop the capability for running the PISA (PHENIX Integrated Simulation Application) detector simulation program (from Professor C. Maguire of Vanderbilt) and install a UNIX version of it on the network of UNIX workstations at ISU. Dr. Petridis found it necessary to develop modifications to the code to make it produce data suitable for the trigger algorithms we had developed.

The modified PISA code has been used so far to examine the performance of two PHENIX detector subsystems - the Muon ID and the RICH. For the Muon ID, simulations were run to determine the minimal number of detection planes that need to be instrumented, and the optimal location of these planes. When the choice of 3 active planes was made by the collaboration, the simulations were used to determine the efficiency of muon detection as a function of muon energy. We found out that the muon acceptance of the muon detector begins to drop sharply as the muon energy falls below 2 GeV.

The trigger level-1 algorithm for the RICH detector uses PMT modules (a module is a 5x5 array of PMTs) in a tiling scheme to detect the Cherenkov rings that are formed on the focal plane of the mirrors of the RICH detector. A modification was made to produce from PISA the data needed to test our RICH algorithm. Dr. Petridis then wrote a separate code to test the algorithm as a function of its threshold and the position of an electron ring on the RICH array. This required developing a code to generate an isotopic distribution of single electrons over an arm of the RICH detector. The original RICH algorithm was evaluated by use of these simulations, which suggested an extension to the original algorithm to provide a nearly perfect 100% counting of single electrons with essentially no overcounting. (Without the extension, overcounting of electrons was unacceptably large and could have misled the RICH level-1 trigger into thinking an event had two electrons when only one actually hit the RICH.) This significant improvement of the RICH algorithm could not have been readily deduced without the trigger simulation tests.

Additional tests of the RICH algorithm are currently nearing completion. They involve testing the high transverse-momentum limit of the RICH level-1 trigger algorithm to resolve and count two closely spaced electrons. We need to know the maximum transverse momentum that a particle, such as a vector meson, can have such that its decay into an e^+e^- pair is detected by the RICH detector. In this case, the high transverse-momentum limit implies a minimum opening-angle for the RICH level-1 algorithm. The tests, although as yet incomplete, indicate no difficulty until transverse momenta above about 20 GeV/c are reached for the J/ψ meson. This is large enough not to be a significant factor in using the RICH to study the e^+e^- decays of the vector mesons. The sensitivity of this result to magnetic effects and the event position in the interaction diamond will soon be evaluated.

4. Progress in PHENIX Tracking

We have participated in the studies of the PHENIX Tracking group, for which Ed O'Brien (BNL) is the spokesman. We participated in the AGS test beam run in June 1992 of the TEC (Time Expansion Chamber) which was run in the dE/dx mode and also as a TRD (Transition Radiation Detector) after being loaded with polypropylene foils. A TEC can detect electrons produced either by ionization (i.e., the usual dE/dx signal that is spread out over the entire path of the charged particle in the gas of the detector) or by the electron "burst" due to a TR photon. (A burst occurs because the photon of several keV is absorbed at a specific point along the path of the charged particle in the detector.) The TEC used in the 1992 test beam run could not be optimized simultaneously for both ionization and TR detection, but provided useful data for designing a new, thicker TEC.

Three new, thicker TECs will be ready for use in the June 1993 test beam run at the AGS. We (Hill and Wohn) plan to participate in this run by taking shifts during the run. In addition, Dr. Bruce Libby, who is our postdoc stationed at BNL, and Mr. Lars Ewell, a graduate student who will be at BNL from April through July 1993, have been working with Ed O'Brien and the TEC chambers. Mr. Ewell has been assisting in assembling and preparing the new TEC chambers for the test beam run.

Dr. Libby has assisted with TEC assembly but he has concentrated on simulating the performance of the chambers using the GARFIELD code, which is a CERN library program that calculates electron and positive-ion drift path, drift times, and the signals induced on the sense wires by a minimum ionizing particle. GARFIELD has been used to monitor changes in the drift path, drift times, and the sense-wire signals as the potential in both the drift and proportional regions is changed. In addition, the effects of changing the gas in the TEC, using a variety of gas mixtures based on Ar and Xe, were studied with GARFIELD. The signals calculated by GARFIELD can be convoluted with response functions to simulate the signals from preamplifiers and shapers. In this manner GARFIELD provides a reasonable approximation to the expected output of the TEC, which, when compared with the actual test beam data, will be an important tool to be exploited in the design of the final TEC for PHENIX.

B. Participation in E864 at the AGS Accelerator

In March 1993 the Iowa State group was invited to join E864, which is scheduled to begin taking data at the AGS in the summer of 1994. The purpose of this experiment is conveyed in the title "Measurement of Rare Composite Objects and High Sensitivity Searches for Novel Forms of Matter Produced in High Energy Heavy Ion Collisions". We are particularly interested in the search for "strangelets" or other forms of strange matter and antinuclei. This will also give us an opportunity to gain experience in a large-scale relativistic heavy ion experiment prior to running at RHIC and to do some interesting physics.

Our role in E864 is already very well defined. We are responsible for designing and building the late-energy trigger. Our experience with the level-1 trigger at PHENIX and the availability of the expertise of the Ames Laboratory Engineering Services Group make this role a natural for our group. Also the late-energy trigger will not be implemented until 1995 which is convenient for us since we only recently joined the collaboration. Although our group has the lead responsibility for the late-energy trigger, we will be assisted by a group from Purdue University that also recently joined E864.

In E864 it is not possible to reach the desired level of sensitivity (1 part in 10^{11}) for the rarest events without a very selective trigger. A very restrictive trigger condition is that an event is accepted only if it hits the calorimeter at least 2.5 ns after a speed-of-light particle and if it deposits a minimum of 3 GeV in one tower of the calorimeter. Fortunately this condition should be met by the rarest events of interest such as stranglets, antideuterons, antitritons, and the heavier nuclear systems. A first design for the late-energy trigger has been proposed by our group and presented to the E864 collaboration at the collaboration meeting in May 1993. The preliminary design for the trigger is shown in Fig. 1. The trigger operates in the following manner. The output from each of 616 towers of the calorimeter is fed to an integrator that produces an energy signal. Each tower output also passes through a discriminator that is used as a stop for a TAC. The TAC is started by a signal from the multiplicity counter located near the target. The time information from each TAC and the energy information from each

individual detector are fed to a lookup table which gives an output if the late-energy criterion is met. The outputs from the 616 lookup tables are fed to an OR which produces a trigger if a yes is obtained from any one of the 616 channels. The total time needed to produce a trigger is of the order of 100 ns.

C. Studies of Electromagnetic Dissociation (ED)

Late in the 1970s, after Heckman and Lindstron observed ED at the Bevalac, we realized that the electromagnetic fields generated at the nucleus in relativistic heavy ion (RHI) reactions with high-Z nuclei could become extremely large. A major effort of our program has been to study the charge dependence of the ED process using projectiles with energies between 1 and 2 GeV/nucleon from the Bevelac. The ED cross section is expected to rise dramatically as the charge of the projectile is increased. We thus carried out an experiment under Bevelac proposal 878H to measure ED cross sections on ^{197}Au and ^{59}Co targets using 0.96 GeV/nucleon ^{238}U beams.

Our value for the ED cross section for ^{197}Au(^{238}U,X)^{196}Au is 3.16 barns. This is the largest ED cross section yet observed but is significantly smaller than the value of 4.05 barns calculated by us using the Weizsacker-Williams (WW) virtual photon method. Our result for ^{197}Au may mean that the ED cross section increases more slowly with projectile charge than previously expected, which is good news for builders of the next generation of relativistic heavy ion accelerators such as RHIC. A letter presenting the Au results has been published in Physics Letters and a longer paper describing in detail the ^{238}U experiments has been submitted to Physical Review C.

In addition to studying the ED charge dependence, we are studying the ED energy dependence by experiments at the AGS Heavy Ion Facility (Exp. 819) and the CERN-SPS accelerator (Exp. NA40). The experiments were carried out at the AGS accelerator using 13.4 GeV/nucleon ^{16}O and ^{28}Si projectiles on ^{197}Au and ^{59}Co targets. The CERN-SPS experiments involved 200 GeV/nucleon ^{16}O and ^{32}S and 60 GeV/nucleon ^{16}O projectiles on ^{197}Au targets. Counting of radioactivities from the above bombardments has been completed at Ames and final data analysis is nearing completion.

Calculations using the WW method indicate that σ_{ED} can become very large for high-Z projectiles at ultrarelativistic energies. At the energy of 100 GeV/nucleon planned for the RHIC collider, we calculate for the reaction ^{197}Au(^{197}Au,X)^{196}Au that σ_{ED} reaches 56 b for colliding beams. The first opportunity to study large σ_{ED} was in the spring of 1992 when ^{197}Au beams from the AGS became available. Our AGS Proposal E862, entitled "Electromagnetic Dissociation of ^{59}Co and ^{197}Au Projectiles," (approved in June 1990 for 36 hours of beam time) pointed out that our WW calculations indicate for ^{197}Au(^{197}Au,X)^{196}Au a σ_{ED} of 10 barns for 11 GeV/nucleon ^{197}Au beams.

LATE ENERGY TRIGGER 5/20/93
E864

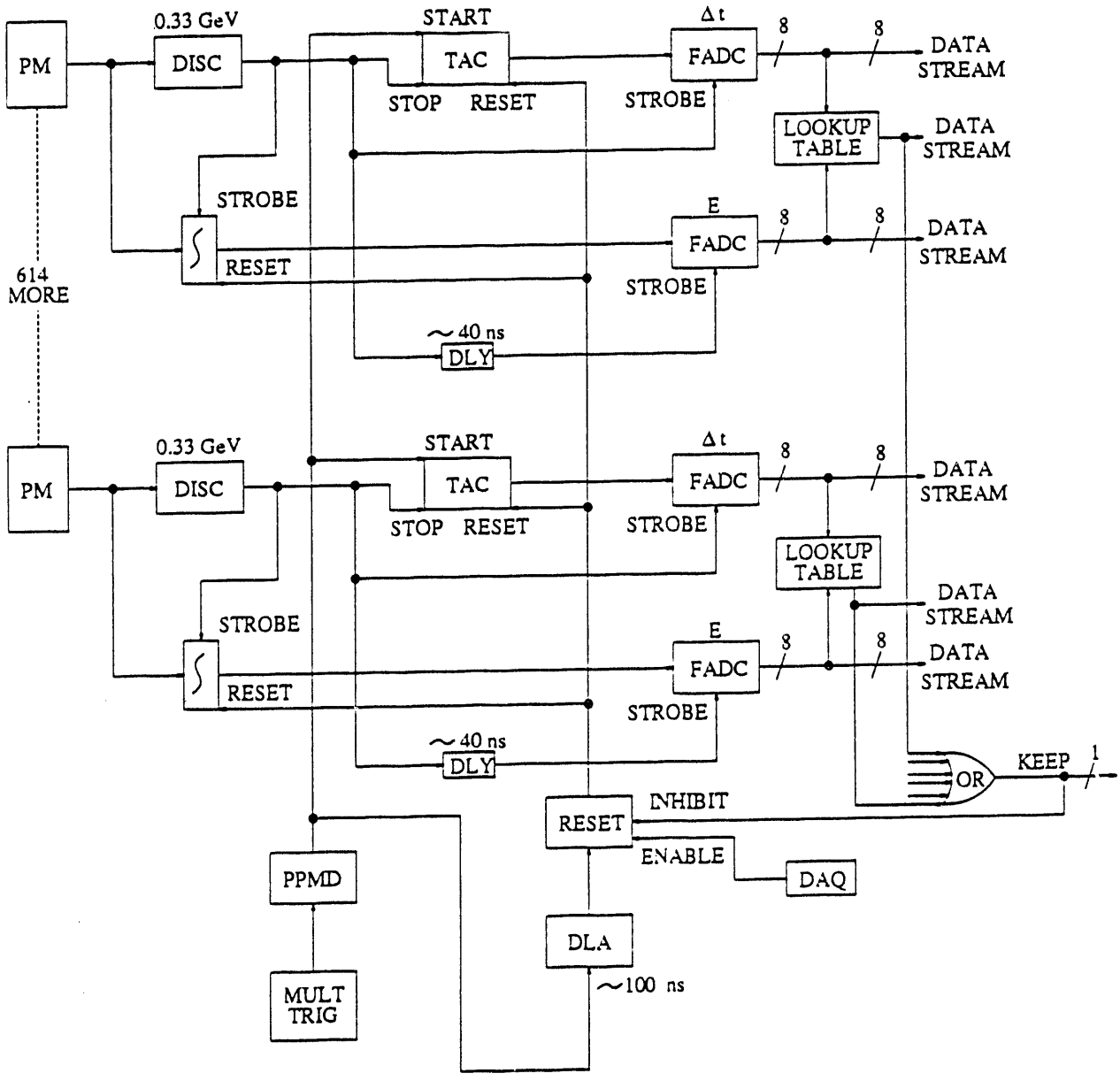

FIG. 1. Preliminary design for E864 late energy trigger.

For our AGS experiment E862, the bombardments with the ^{197}Au beam were completed in April 1992 and counting of the bombarded ^{197}Au and ^{59}Co targets is in progress at Ames using techniques developed by us for earlier ED experiments. Due to the large σ_{ED} expected, a few changes were made in the bombardment sequence. We determined the total cross section for the ^{197}Au(^{197}Au,X)^{196}Au reaction by counting individual beam particles at reduced beam intensity using a two-element counter telescope. Separate runs at maximum intensity were carried out in order to measure cross sections for deep spallation products needed to determine the nuclear contribution to the total cross section. After looking at preliminary results we judged that the high-intensity portion of the experiment was successful but that it would be useful to obtain more data at low beam intensities. Additional running of our experiment using the Au beam at the AGS has been approved for September 1993. Mr. Lars Ewell, a graduate student in our group, will earn his Ph.D. working on this project.

We collaborated with GSI colleagues on experiment SO32, entitled "Inclusive Measurements of Electromagnetic Dissociation Cross Sections", whose spokesman is K. Summerer of GSI. The run was carried out at GSI in June 1991 on the SIS accelerator using 1 GeV/nucleon ^{197}Au beams. The techniques used for bombardment and data analysis were based on those worked out by our group for experiments at the Bevelac. The results were published in Phys. Rev. C (see publication lists). At the present time we do not anticipate carrying out additional experiments at GSI on ED.

D. Completion of Nuclear Structure Studies

Our last studies at the TRISTAN separator at the HFBR in Brookhaven were focused on the A=100 region of deformed nuclei. We concentrated on measurements of level lifetimes using the Fast Electronic Scintillator Timing (FEST) system to measure the E2 and M1 moments of excited states of neutron-rich nuclei in this region. Using the E2 and M1 moments we were able to respectively deduce the deformation and magnetic g-factors of the low-lying rotational bands. Our final study in the A=100 region involved the E2 strength of the first-excited 2^+ state in the spherical even-even Sr nuclei with A=90-96. Combining these results with the E2 strengths of the deformed Sr nuclei with A=97-100, revealed that the shape transition from spherical to deformed for neutron-rich Sr nuclei is so exceptionally large and abrupt that it suggests a "phase change" in the collectivity of the Sr nuclei. No other nuclear region exhibits such an abrupt change in nuclear collectivity with particle number. Because of our report on this unique phenomenon, Dr. Wohn was asked to give an invited talk at the symposium on "Nuclear Shapes" at the August 1992 meeting of the American Chemical Society in Washington, D.C.

The Ph.D. thesis research of Mr. Vo, one of our graduate students, involves the study of high angular momentum states in heavy nuclei (A=190-198) using the High Energy Resolution Array (HERA) at the 88 cyclotron at Berkeley. These studies are done in collaboration with scientists from Berkeley, Livermore, Orsay, and U.C. Davis. Mr. Vo was in residence at Berkeley for most of 1992 and obtained all of the data needed for his PhD thesis before HERA was decommissioned in 1992. His thesis will describe a new

Superdeformed (SD) band that he observed in an isotope of Au using ^{11}B projectiles on a ^{186}W target. The new SD band has been tentatively assigned to ^{191}Au on the basis of the excitation function results and is the first to be observed in Au (Z=79). This extends for the first time this region of superdeformation below Z=80. The gamma-ray energies in this new SD band in ^{191}Au are similar to those in an excited SD band of ^{191}Hg. This work has been submitted to Physical Review Letters. In addition, Mr. Vo gave an oral presentation of his work in April 1993 at the Spring meeting of the American Physical Society.

The HERA facility at Berkeley was also used by Mr. Vo to search for resonant states in e^+e^- scattering via their predicted 2 and 3 photon decay modes. This project also involved Professor William Kelly of ISU as well as several of their colleagues in the SD studies. (Such resonant states, called photonium, have been predicted by Professor James Vary and Dr. John Spence of ISU.) For the 2 and 3 photon decay searches, HERA was used offline. Two positron sources were located in hollow spheres, one Pb and the other Cu, either of which were placed at the center of HERA. Each sphere contained about 0.1 mCi of ^{68}Ga (in secular equilibrium with 288-d ^{68}Ge). The predicted procedure for the formation of photonium states was that positrons from the ^{68}Ga decay with energies up to 1.9 MeV would lose energy in the target spheres, and, when their energy passed through a resonant energy, interact with an electron in the target spheres to form photonium. The HERA facility could then be able to detect the 2 and 3 gamma decay modes. After 100 days of data (mostly taken with the Pb sphere) there was no indication of photonium states. Upper limits were placed on the partial widths for the 2 and 3 photon decay modes. This work has very recently been submitted to Physical Review C.

PUBLICATIONS

Published (Journals)

T. Aumann, J. V. Kratz, E. Stiel, K. Sümmerer, W. Brückle, M. Schädel, G. Wirth, M. Fauerbach, and J. C. Hill, "Inclusive Measurements of Electromagnetic Dissociation of ^{197}Au Targets," Phys. Rev. C **47**, 1728 (1993).

K. E. Lassila, A. N. Petridis, U. P. Sukhatme, and G. Wilk, "Shadowing of the Gluon in Fixed Target Experiments" Phys. Lett. B **297**, 191 (1992).

P. Roussel-Chomaz, N. Colonna, Y. Blumenfeld, B. Libby, G. F. Peaslee, D. N. Delis, K. Hanold, M. A. McMahon, J. C. Meng, Q.C. Sui, G. J. Wozniak, L. G. Moretto, H. Madani, A. A. Marchetti, A. C. Mignerey, G. Guarino, N. Santoruvo, I. Iori, and S. Bradley, "Complex Fragment Production and Multifragmentation in ^{139}La-induced Reactions at 35, 40. 45, and 55 MeV/u" Nucl. Phys. **A551**, 508 (1993).

Published (Proceedings)

J. C. Hill, F. K. Wohn, D. D. Schwellenbach, and A. R. Smith, "Coulomb Dissociation in Relativistic Heavy Ion Reactions," in Relativistic Aspects of Nuclear Physics, edited by T. Kodama, Y. Hama, K. C. Chung, S.J.B. Duarte, and M.C. Nemes, World Scientific Publishing Co., p. 255 (1992). (Invited Talk).

B. Libby, A. C. Mignerey, H. Madani, A. A. Marchetti, P. Roussel-Chomaz, N. Colonna, Y. Blumenfeld, G. F. Peaslee, D. N. Delis, M. A. McMahan, J. C. Meng, L. G. Moretto, G. J. Wozniak, M. Colonna, and M. DiToro, "The Decay of Hot Nuclei formed in La-induced Reactions at Intermediate Energies," Proceedings of the Eighth Winter Workshop on Nuclear Dynamics, Jackson Hole, WY, January 18-24, 1992, edited by W. Bauer and B. Back, World Scientific, Singapore (1992).

Submitted

D. T. Vo, W. H. Kelly, F. K. Wohn, J. C. Hill, M. A. Deleplanque, R. M. Diamond, F. S. Stephens, J. R. B. Oliveira, J. Burde, A. O. Machiavelli, J. deBoer, J. A. Becker, E. A. Henry, M. J. Brinkman, A. Kuhnert, M. A. Stoyer, J. R. Hughes, J. E. Draper, C. Duyar, and E. Rubel, "Superdeformation in ^{191}Au," Phys. Rev. Lett.

D. D. Schwellenbach, J. C. Hill, F. K. Wohn, P. R. Graham, A. R. Smith, D. L. Hurley, C. J. Benesh, and P. J. Karol, "Electromagnetic Dissociation of ^{59}Co and ^{197}Au Targets by Relativistic ^{238}U Projectiles", Phys. Rev. C.

D. T. Vo, W. H. Kelly, F. K. Wohn, J. C. Hill, J. P. Vary, M. A. Deleplanque, R. M. Diamond, F. S. Stephens, J.R.B. Oliveira, A. O. Macchiavelli, J. A. Becker, E. A. Henry, M. J. Brinkman, M. A. Stoyer, and J. E. Draper, "Search for Multi-Photon Final-State Resonances in Low-Energy e^+e^- Scattering," Phys. Rev. C.

A. N. Petridis, K. E. Lassila, and J. P. Vary, "Direct Photon Production in Heavy Ion Collisions", Phys. Rev. D.

A. A. Marchetti, A. C. Mignerey, H. Madani, A. Gokmen, W. L. Kehoe, B. Libby, K. Morley, H. Breuer, K. Wolf, and F. Obenshain, "Mass and Charge Distributions in Cl-induced Nuclear Reactions" Phys. Rev. C.

Invited Talks

F. K. Wohn, "Level Lifetimes and Shape Transitions for A=100 Nuclei," Symposium on Nuclear Shapes, American Chemical Society Meeting, Washington, DC, August, 1992.

J. C. Hill, "Birth of the Universe, Recreated", afterdinner talk at meeting of South Dakota High School Teachers, Pierre, SD, October 1992.

B. Libby, "The Decay of Hot Nuclei Formed in La-Induced Reactions at E/A=45 MeV", Nuclear Seminar, Argonne National Laboratory, Argonne, IL, December 1992.

J. C. Hill, "Electromagnetic Dissociation in Relativistic Heavy Ion Collisions", Nuclear Seminar, Purdue Univ., W. Lafayette, IN, April 1993.

Contributions

A. Bouchard, F. C. Peterson, and F. K. Wohn, "Recent Efforts to Improve the Classroom Performance of Teaching Assistants," AAPT Announcer, **22**, 53 (1992).

D. T. Vo, W. H. Kelly, F. K. Wohn, J. C. Hill, M. A. Deleplanque, R. M. Diamond, F. S. Stephens, J.R.B. Oliveira, J. Burde, A.O. Machiavelli, J. deBoer, J. A. Becker, E.A. Henry, M. J. Brinkman, A. Kuhnert, M.A. Stoyer, J.R. Hughes, J.E. Draper, C. Duyar, and E. Rubel, "Superdeformation in ^{191}Au," BAPS **38**, 1049 (1993).

B. Libby, A. C. Mignerey, H. Madani, A.A. Marchetti, Y. Blumenfeld, N. Colonna, D. N. Delis, M.A. McMahan, J. C. Meng, L. G. Moretto, G. F. Peaslee, P. Roussel-Chomaz, X. Sui, G. J. Wozniak, and S. Bradley, "Study of the Decay of Hot Nuclei Formed in La-induced Reactions at E/A=45 MeV" BAPS **37**, 985 (1992).

APPENDIX

Table 11.6: Interaction rates, time between events and data volumes for events satisfying various criteria for selecting one and two $e^{\pm}$.

Beams	Type	Prob. Any Pair	T_{avg} (μs)	MB/s	Prob. E>.4 GeV	T_{avg} (μs)	MB/s	Prob. True Pair	kB/s
p + p	MB	$2.4\ 10^{-4}$	9200	0.22	$7.0\ 10^{-4}$	3150	0.61	$9.4\ 10^{-7}$	0.82
O + O	MB	$2.1\ 10^{-3}$	2630	2.47	$3.5\ 10^{-3}$	1600	3.63	$4.7\ 10^{-6}$	4.79
Si + Si	MB	$5.5\ 10^{-3}$	1530	7.50	$6.5\ 10^{-3}$	1300	7.68	$8.4\ 10^{-6}$	9.87
Cu + Cu	MB	$2.1\ 10^{-2}$	999	26.60	$1.6\ 10^{-2}$	1350	16.80	$2.2\ 10^{-5}$	24.10
I + I	MB	$6.5\ 10^{-2}$	658	84.10	$3.3\ 10^{-2}$	1310	36.10	$4.7\ 10^{-5}$	52.70
Au + Au	MB	$1.3\ 10^{-1}$	569	154.00	$5.2\ 10^{-2}$	1390	54.80	$7.5\ 10^{-5}$	80.40
p + p	Cn	$3.5\ 10^{-3}$	63700	0.08	$5.9\ 10^{-3}$	37200	0.14	$8.1\ 10^{-6}$	0.19
O + O	Cn	$1.1\ 10^{-2}$	5200	1.90	$1.3\ 10^{-2}$	4470	2.21	$1.6\ 10^{-5}$	2.84
Si + Si	Cn	$2.9\ 10^{-2}$	2960	5.90	$2.3\ 10^{-2}$	3650	4.77	$3.0\ 10^{-5}$	6.20
Cu + Cu	Cn	$1.1\ 10^{-1}$	1960	20.90	$5.5\ 10^{-2}$	3870	10.60	$8.1\ 10^{-5}$	15.80
I + I	Cn	$3.1\ 10^{-1}$	1370	63.90	$1.1\ 10^{-1}$	3820	23.00	$1.7\ 10^{-4}$	33.70
Au + Au	Cn	$5.9\ 10^{-1}$	1220	116.00	$1.8\ 10^{-1}$	4030	35.10	$2.6\ 10^{-4}$	51.60
p + O	MB	$3.4\ 10^{-4}$	7310	0.32	$9.3\ 10^{-4}$	2680	0.84	$1.2\ 10^{-6}$	1.11
p + Si	MB	$4.0\ 10^{-4}$	6170	0.42	$1.1\ 10^{-3}$	2350	1.04	$1.4\ 10^{-6}$	1.38
p + Cu	MB	$5.1\ 10^{-4}$	5650	0.51	$1.3\ 10^{-3}$	2280	1.20	$1.7\ 10^{-6}$	1.60
p + I	MB	$6.5\ 10^{-4}$	5110	0.64	$1.5\ 10^{-3}$	2190	1.40	$2.0\ 10^{-6}$	1.89
p + Au	MB	$7.6\ 10^{-4}$	4770	0.75	$1.7\ 10^{-3}$	2130	1.55	$2.3\ 10^{-6}$	2.11
Si + Cu	MB	$2.5\ 10^{-2}$	522	56.70	$1.7\ 10^{-2}$	749	33.80	$2.5\ 10^{-5}$	48.80
Si + I	MB	$3.2\ 10^{-2}$	557	62.10	$2.1\ 10^{-2}$	874	33.80	$2.9\ 10^{-5}$	49.10
Si + Au	MB	$3.7\ 10^{-2}$	604	62.60	$2.2\ 10^{-2}$	994	32.40	$3.2\ 10^{-5}$	47.20

11.3.3 Level-1 Trigger

Overview

The PHENIX Level-1 (LVL-1) trigger determines for each bunch crossing whether or not an interaction occurred, and if so, whether or not the interaction should be digitized and passed on to the LVL-2 trigger system. The LVL-1 scheme chosen provides a deadtimeless, pipelined, parallel trigger operating in synchronism with the BC clock and delivering at each BC decisions and output data for the BC occurring a fixed time earlier. The LVL-1 trigger also provides hit-pattern information that may be used to direct zero-suppression algorithms and LVL-2 trigger processing for some of the detector subsystems. The LVL-1 trigger will be used to enhance the rate of less common events relative to the minimum-bias rate by setting

Table 11.7: Interaction rates, time between events and data volumes for events satisfying various criteria for selecting one and two $\mu^{=}$.

Beams	Type	Prob. Any Pair	T_{avg} milli-s	MB/s	Prob. True Pair	kB/s
p + p	MB	$3.3\ 10^{-6}$	666	0.003	$1.4\ 10^{-6}$	1.29
O + O	MB	$5.5\ 10^{-5}$	102	0.068	$7.5\ 10^{-6}$	7.72
Si + Si	MB	$1.7\ 10^{-4}$	49	0.250	$1.4\ 10^{-5}$	16.70
Cu + Cu	MB	$9.2\ 10^{-4}$	23	1.230	$3.3\ 10^{-5}$	35.20
I + I	MB	$3.9\ 10^{-3}$	11	5.490	$7.2\ 10^{-5}$	80.70
Au + Au	MB	$9.7\ 10^{-3}$	7	13.100	$1.2\ 10^{-4}$	126.00
p + p	Cn	$8.2\ 10^{-5}$	2680	0.002	$1.4\ 10^{-5}$	0.32
O + O	Cn	$3.3\ 10^{-4}$	168	0.059	$2.6\ 10^{-5}$	4.59
Si + Si	Cn	$1.1\ 10^{-3}$	80	0.220	$5.1\ 10^{-5}$	10.50
Cu + Cu	Cn	$5.7\ 10^{-3}$	37	1.110	$1.2\ 10^{-4}$	22.60
I + I	Cn	$2.4\ 10^{-2}$	18	4.980	$2.6\ 10^{-4}$	53.00
Au + Au	Cn	$6.1\ 10^{-2}$	12	11.900	$4.2\ 10^{-4}$	82.80
p + O	MB	$5.5\ 10^{-6}$	456	0.006	$2.0\ 10^{-6}$	1.82
p + Si	MB	$6.8\ 10^{-6}$	365	0.008	$2.3\ 10^{-6}$	2.27
p + Cu	MB	$9.2\ 10^{-6}$	314	0.010	$2.8\ 10^{-6}$	2.67
p + I	MB	$1.2\ 10^{-5}$	269	0.013	$3.4\ 10^{-6}$	3.16
p + Au	MB	$1.5\ 10^{-5}$	242	0.016	$3.8\ 10^{-6}$	3.54
Si + Cu	MB	$1.1\ 10^{-3}$	12	2.750	$3.7\ 10^{-5}$	71.10
Si + I	MB	$1.6\ 10^{-3}$	12	3.220	$4.4\ 10^{-5}$	72.30
Si + Au	MB	$1.8\ 10^{-3}$	12	3.370	$4.8\ 10^{-5}$	70.00

thresholds or windows on energy sums and particle counts in various detectors or by requiring particle-specific detectors like the EMCal, RICH, or μID to fire. The trigger decision will be made using analog signals, digitized data, and hit-pattern information supplied to the LVL-1 trigger by many detectors. PHENIX is interested in a wide variety of physics observables, which means the LVL-1 trigger must be able to test the various conditions in parallel because of the requirement of deadtimeless operation of LVL-1. All results from LVL-1 become available simultaneously after a fixed time latency. This requirement helps insure future expandability of LVL-1. Pre-scalers will be used for each trigger condition so that common or minimum bias events can be collected in parallel with rare events without the event rate saturating the throughput of the system. The pre-scalers also provide control over the mix of events passed on to the LVL-2 trigger system. Because the LVL-1 decision must be made for each bunch crossing and because the decision cannot be made within the crossing period, the

LVL-1 processing must be pipelined, with a latency currently chosen to be 32 BC. Detectors whose response is slower than this fixed latency cannot be used to make decisions at LVL-1.

The LVL-1 decision process can be divided into three logical stages. The first stage produces flash-digitized data from some of the detectors (e.g., BB counters) and discriminator output signals for the rest of the detectors. The next processing stage, called Local LVL-1 (LL1), performs subdetector-specific calculations that, for example, produce EMcal energy sums, a count of EMcal towers above specified energy cuts, a count of rings in the RICH, and charged-particle multiplicities in the MVD. The last stage of LVL-1 analysis, the Global LVL-1 trigger (GL1), applies user-specified cuts and logical conditions to various parameters to produce a set of LVL-1 trigger results, applies the chosen pre-scale factors to each of the satisfied conditions and returns a final LVL-1 trigger decision. In the current design, approximately 82,000 bits of data are produced by the first stage of LVL-1 processing and passed to LL1. The LL1 processing of all subsystems produces a combined 16,000 bits of output data, about 10% of which are passed to GL1. If the event is accepted by the LVL-1 trigger, the full set of 16K bits are formatted and added to the event stream and passed to LVL-2 and the main event data stream. There are varying numbers of internal steps in the processing pipelines for the various subsystems LL1 systems. The data produced by the subsystem LL1 systems are re-synchronized in FIFO buffers before being transferred to GL1 and the event stream. The current design of the LVL-1 trigger has 140 bits of data fed to GL1.

The block diagram for the overall LVL-1 trigger scheme is shown in Fig. 11.30. In the figure the subsystems contributing to the LVL-1 trigger decision are shown to the far left. The final outputs of the LVL-1 trigger system are shown at the far right. The flow in time is from left to right. Currently, the LVL-1 trigger design uses information from six of the PHENIX subsystems, namely BB, MVD, TOF, RICH, EMCal, and μID. The number of inputs from the subsystems to the LVL-1 trigger processors are shown along with the number of bits for each input. The volume of control information and data passed to the data stream from each detector subsystem is shown on the right, given as (# items)$\times$(# bits/item). As shown in Figure 11.30, four additional signals are provided to GL1. These four inputs indicate whether each of the right and left beam buckets are empty, whether a calibration is being carried out, and whether there is room in the buffers used to store the results of the LVL-1 processing.

A basic building block used in LVL-1 is a pipelined digital summing tree. This is shown schematically in Fig. 11.31 for the case of eight 6-bit inputs being summed to produce a single 9-bit output. Each stage of this summing tree is active for any given beam crossing, with successive stages handling successive events. The BC clock is used to move data through this structure, ensuring that time synchronism is maintained for all events.

The following sections describe in more detail the interface between LVL-1 and the various detector subsystems providing data to LVL-1, the analysis of this data carried out by LVL-1, and the current design for implementing programmable selection logic to generate the actual triggers.

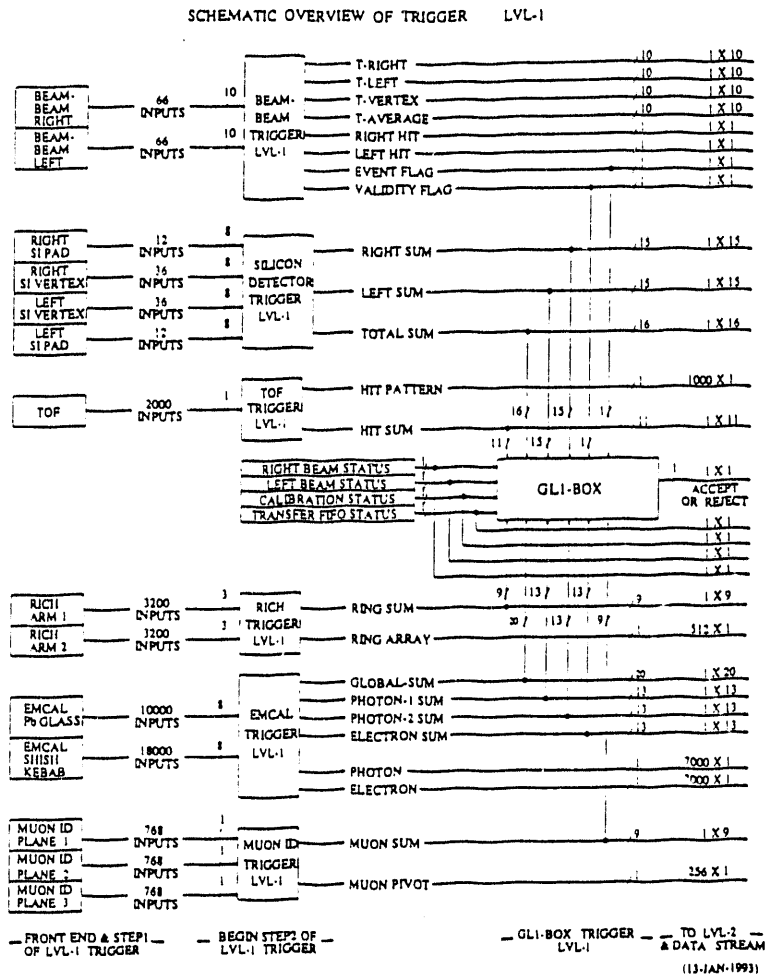

Figure 11.30: Schematic diagram of overall LVL-1 trigger scheme. (The number of bits is the number shown above the symbol "/".)

Beam-Beam

The data from the Beam-Beam counters (BB) provide the least-biased LVL-1 trigger for A+A and p+A collisions, provide rejection against interactions that occur in the ends of or outside of the interaction diamond (especially beam-gas events), and provide a fast time-zero reference (T0) for time-of-flight analyses performed at LVL-2. We must be able to accept events when only one of the arrays fires, because in p+A collisions the array opposite the incoming proton beam frequently will not see any particles. No vertex or T0 information can be obtained at LVL-1 for these events.

As described in Chapter 5, BB is composed of two arrays of 66 "flash-light" Cherenkov detectors. If any valid (see below) hit is found in at least one element in the left or right BB arrays, then that array is considered as having fired. The LL1 analysis for the Beam-Beam system determines whether each of the left and right arrays was hit, and for each end that

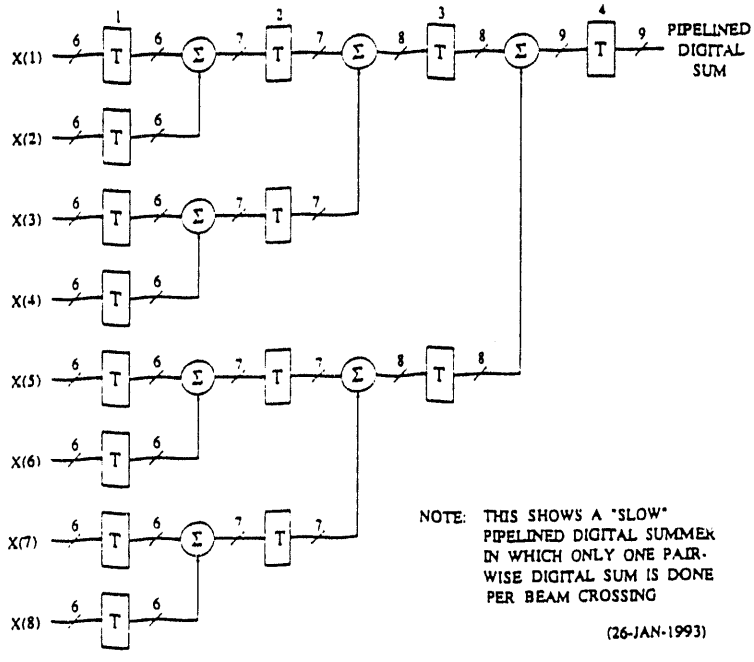

Figure 11.31: Pipelined digital summing tree.

was hit, determines the measured time relative to the arrival of the accelerator RF clock pulse. The time for each array is taken to be the earliest time (within certain limits) from all of the elements of each array with valid hits. If both arrays are hit, an average time and vertex position are returned also.

The LVL-1 system needs time measurements from the BB counters on each bunch crossing. These times are obtained by flash-digitizing a TAC started with BC and stopped with a discriminator pulse from the counters (see Chapter 5). A 10-bit FADC is used for each element of each array. The counters are run in common-start mode, which means that the

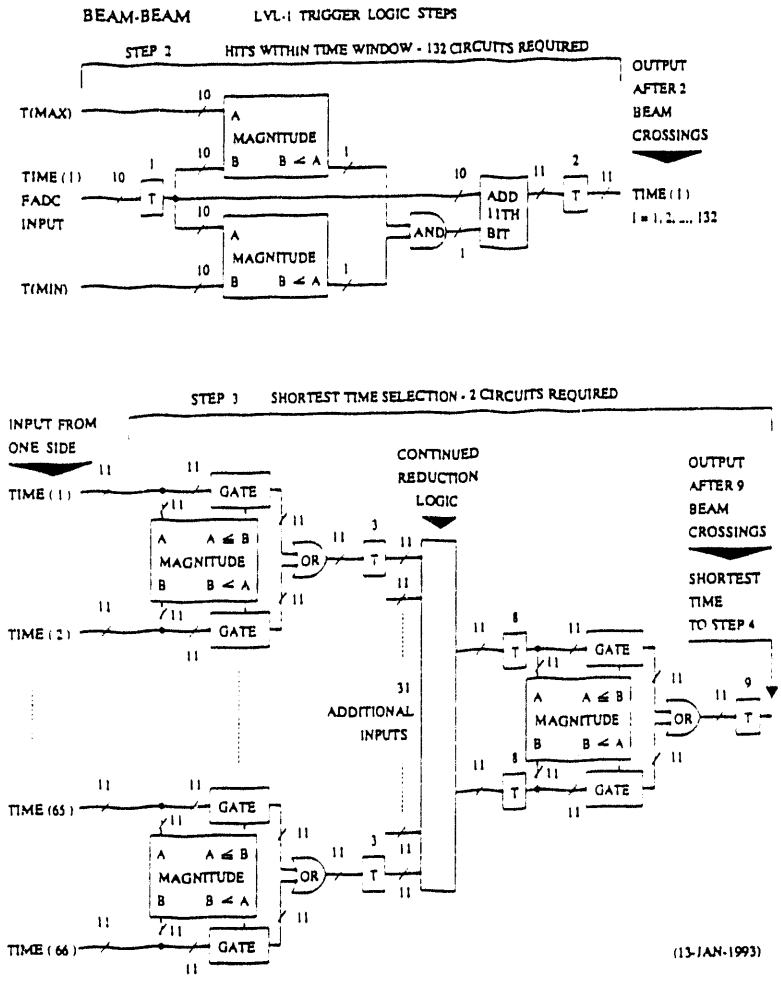

Figure 11.32: Schematic diagram of LVL-1 trigger for Beam-Beam (early stages).

counters which are not hit have extremely late (i.e. overflow) time values. The FADC times are corrected for channel-to-channel cable offsets in the BB front-ends using a fast memory lookup table, whose input address is the FADC output for each detector.

Schematics for different stages of the LL1 processing for the Beam-Beam system are shown in Figs. 11.32 and 11.33. The steps in the Beam-Beam LL1 processing pipeline are described in sequential order below. Also included are the number of bunch crossings (assuming 112 ns) taken by each step in the pipeline.

Step 1 - Flash-digitization and time correction (1 crossing): See previous paragraph. We assume that only 1 bunch crossing time is required.

Step 2 - Element Time Validation (1 crossing): The measured time is compared against preset minimum (T(min)) and maximum (T(max))times. This is performed by the dual comparators marked "magnitude." An extra bit is added to

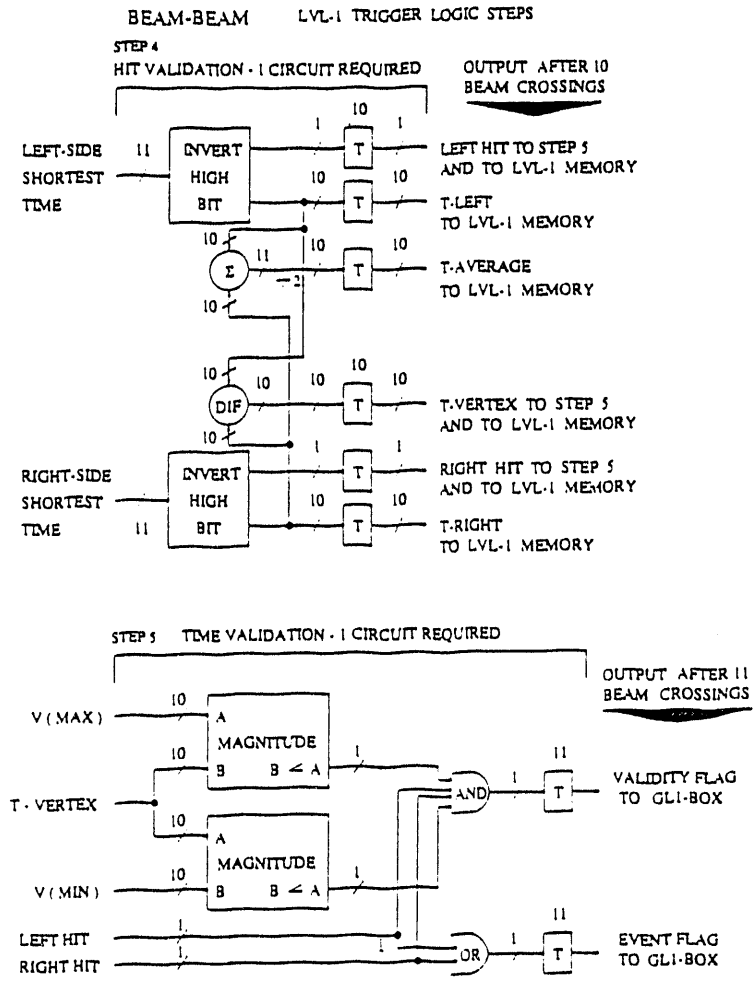

Figure 11.33: Schematic diagram of LVL-1 trigger for Beam-Beam (later stages).

the 10 bits from the Beam-Beam front-ends and is used to indicate whether the measured time is valid. If the hit time is within the specified window, the time is passed to the next stage with the flag (11th) bit cleared. If the time is outside the specified window the flag bit is set. This is useful later if only one array is struck, as is sometimes the case for p+A collisions.

Step 3 - Shortest time selection (7 crossings): The earliest valid time for each array is selected from the detectors in each array. This is done with cascaded comparators, each of which finds the smaller of two numbers. Each stage in the cascade compares a pair of times from the previous stage and passes the smaller. Since a 'set' flag bit produces a large time, if there is any valid hit in an array, it will have a time smaller than the invalid times. which always have the 11th bit set. Thus the valid hits are always selected over any invalid ones.

Step 4 - Array Hit validation (1 crossing): The flag bit is inverted in the left

and right times obtained from Step 3, so it is now set for valid hits. The logic signals indicating the individual status of the two Beam-Beam arrays ("Left-hit" and "Right-hit") are generated. Also, the difference between the the left and right times (vertex position) and the mean of the left and right times (T0) are calculated.

Step 5. Time validation (1 crossing): The vertex position is tested against preset maximum (V(max)) and minimum (V(min)) values, calculated assuming speed-of-light particles. This step provides two output signals, "Event Flag" and "Validity Flag". "Event Flag" is TRUE if either of the two arrays have valid hits. "Validity Flag" is TRUE if both arrays were hit and the vertex is within the preset window. If the validity flag is FALSE, the rough vertex used by LVL-2 must be computed by other means.

The LL1 system for the BB counters produces eight data-words. Four of them, "T-Left", "T-Right", "Event Flag" and "Validity Flag" are 1 bit wide, while the other four data-words, left and right array times, the T0 and the vertex position, are 10 bits wide. The T0 and vertex position are valid if both arrays were hit. Only two of the outputs of the BB LL1 system, "Event Flag" and "Validity Flag," are presented to GL1.

Inner Detectors

The silicon pad and silicon strip detectors, collectively referred to as the Multiplicity/Vertex Detector (MVD), are used at LVL-1 to calculate charged-particle multiplicities measured over a restricted range of pseudo-rapidities. For collisions at $z = 0$ the silicon strip detector covers a pseudo-rapidity range of ± 2.5 and the silicon pad detectors cover the $|\eta|$ range $1.8 - 2.65$. The LVL-1 processing of the MVD data produces charged particle multiplicities summed over subsections of the MVD and a total charged-particle multiplicity for the entire MVD acceptance. The total multiplicity will be used to make a LVL-1 centrality trigger, and the regional multiplicity sums can be used to select events according to left/right criteria.

A schematic diagram of the LL1 processing for the MVD is shown in Fig. 11.34. The steps in the MVD processing pipeline are described in sequential order below along with the number of bunch crossings (assuming 112 ns) taken by each step in the pipeline.

Step 1 - Pad and strip analog summing: The pad and strip detector front ends supply analog sums for each 256-channel sector in the detectors. The analog summing is done on the MVD front-ends and is not shown on the MVD LVL-1 block diagram.

Step 2 - Digitization of Analog Sums (1 crossing): The analog sums are digitized by 8-bit 10 MHz FADCs. The silicon pad detectors produce 24 sums, one for each of their 24 sectors, and the inner layer of the silicon strip detector produces 72 sums, one for each of its sectors.

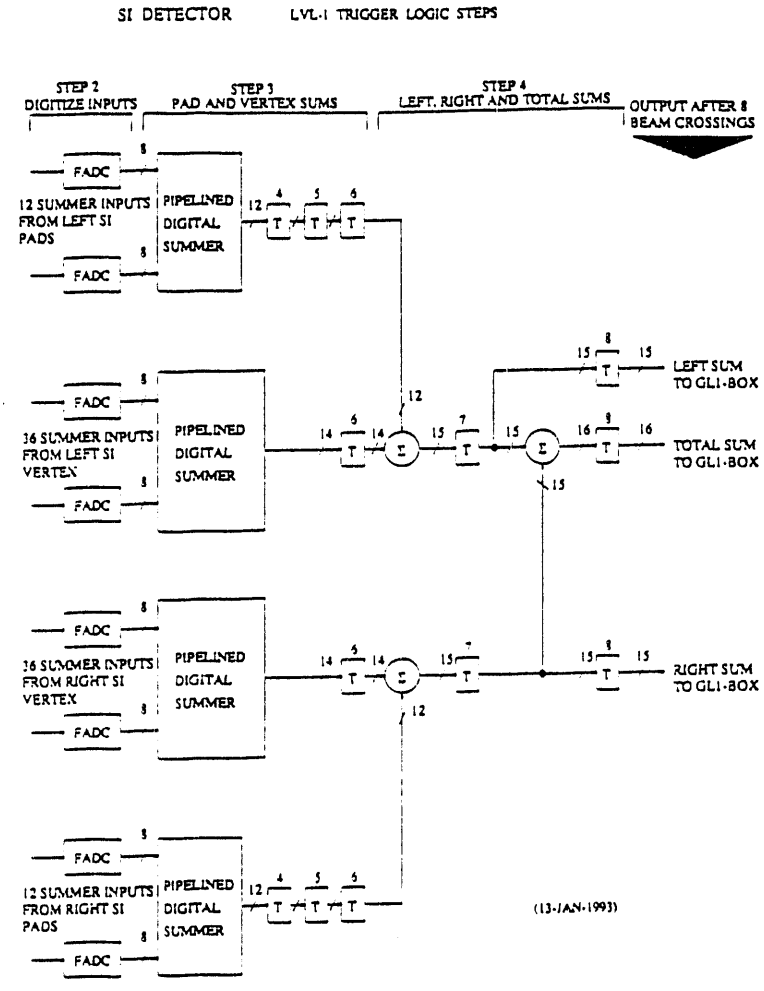

Figure 11.34: Schematic diagram of LVL-1 trigger for MVD.

Step 3 - Regional sums (4 crossings): The digitized sums from the MVD are now digitally summed again to form regional multiplicities. The current design contains multiplicity sums for the left silicon pad detector, the right pad detector, the left side of the inner silicon strip detector, and the right side of the inner strip detector. The sums for the pads complete two time steps sooner and are thus held off for two time steps in order to synchronize with the sums for the strips in Step 4.

Step 4 - Final Multiplicity Sums (2 crossings): The current design produces two 15-bit sums from the sums of step 3. They result from summing the left silicon pad and left silicon strip ("Left-Sum") and right pad and right strip ("Right-Sum") multiplicities. These two sums are then added to produce the total multiplicity ("Total Sum") seen in the MVD. Other combinations of the four multiplicities obtained from Step 3 sums can also be summed in parallel.

These sums become part of the LVL-1 output data stream.

The three final multiplicity sums obtained from the MVD LL1 processing are fed to GL1 where they can be used in conjunction with other GL1 inputs to make a LVL-1 trigger decision. This decision will most often consist of applying one or more thresholds to the multiplicity sums to make centrality cuts.

RICH

The RICH LVL-1 trigger system is designed to find and count Cherenkov "rings" in the RICH. This trigger is critical for triggering on electrons in light-ion collisions because of the high luminosity and low electron rates in these collisions. The ring-finding at LVL-1 also provides the seed locations for ring-finding in the LVL-2 trigger, thus greatly reducing the time the RICH LVL-2 algorithm takes to find and fit rings. The results of the RICH LVL-1 trigger are also used to direct the flow of one set of the electron-finding algorithms in LVL-2; the other set is based on EMCal and PC, as discussed below.

The RICH detector is read out with a 40×80 array of photomultiplier tubes in each of the two arms. For purposes of ring-finding, the array can be thought of as a flat wall with the "horizontal" axis pointing along the beam direction and the "vertical" axis pointing around the detector (ϕ direction). A well-focussed electron ($\beta \approx 1$) ring is fully contained in a 5×5 block of PMTs, including allowance for multiple scattering and geometrical aberrations. To find RICH hits at LVL-1, the RICH imaging area is first divided up into 5×5 arrays of PMTs, called "modules", producing an 8×16 array of modules per arm. In order to find rings which are not centered on a module, the modules are further grouped into "pairs" and "tiles". The pairs are formed both horizontally and vertically and overlap in both directions by one module spacing. The tiles are 2×2 arrays of modules that overlap by a module spacing in both directions. This scheme, demonstrated in Fig. 11.35, therefore puts a single module in four different pairs and four different tiles. There are thus 128 modules, 256 pairs, and 128 tiles per arm.

One final logical grouping of modules, pairs, and tiles is made here to help exposit this tiling scheme. We define a "unit cell" to be composed of a single module, two pairs, and a single tile with the arrangement shown in Fig. 11.35. The unit cell contains all tiling elements that have a given module in their upper-most and left-most corners, so there is a one-to-one mapping between modules and unit cells. There are, then, 128 unit cells overlapped in each direction by one module spacing. The unit cell can be thought of as the logical element containing all rings whose *centers* lie in the shaded region shown in the example unit cell in Fig. 11.35.

The center of a found ring is determined by the type of tiling element (module, pair, or tile) in which it was found. The distribution of centers of those rings which fit completely into modules is centered on the module center. The distribution of centers of rings firing pairs is centered on the mid-point between the modules in a pair. The distribution of centers of rings found in tiles is centered at the mid-point of the tile. The ring centers are indexed by a pair of numbers (k, l), which can be tied to the original modules, as shown in Fig. 11.35. The ring centers with (odd, odd) indices are from single modules, while the centers with (odd,

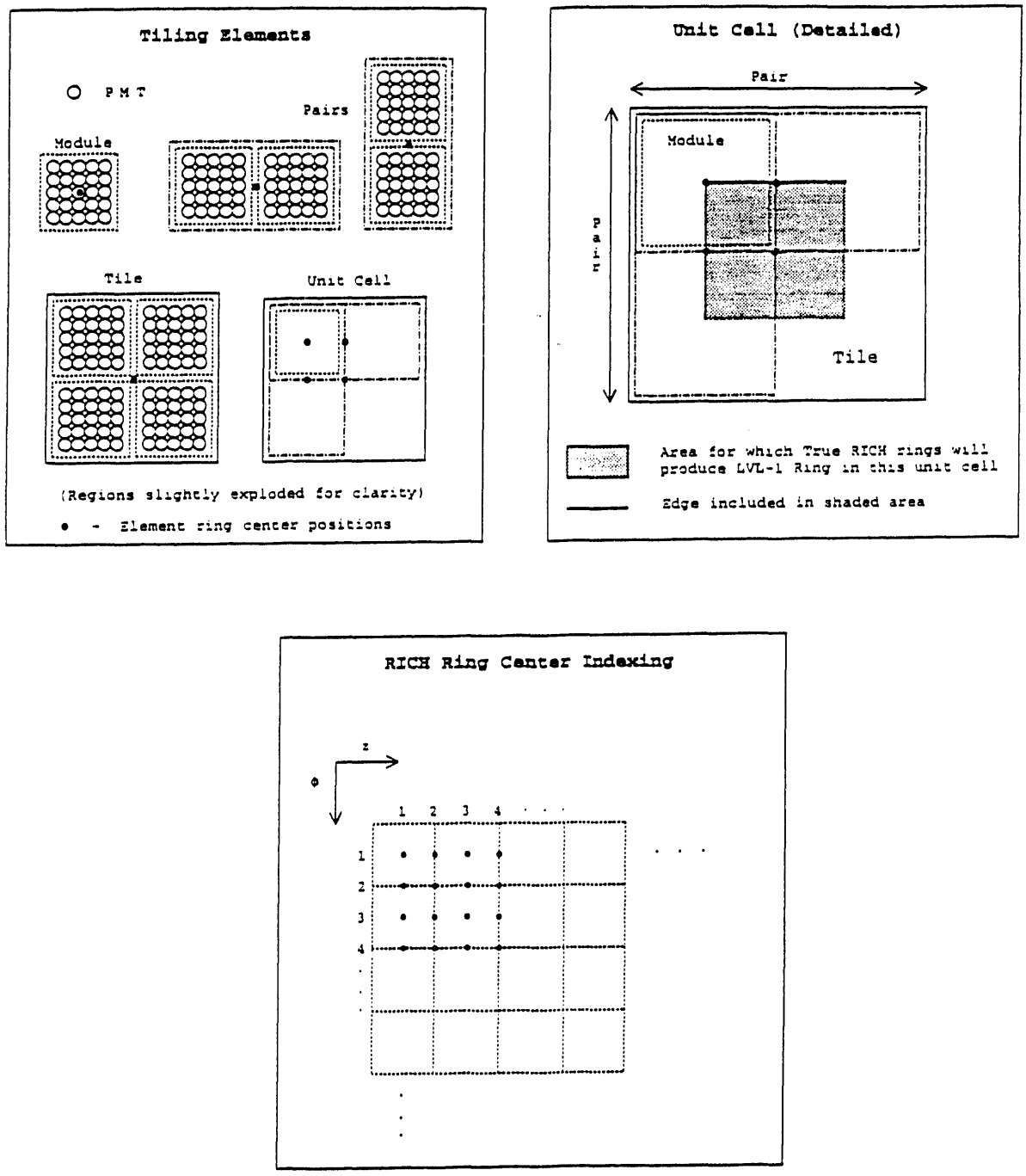

Figure 11.35: Illustration of RICH LVL-1 tiling scheme.

even) or (even, odd) indices are from pairs, and the centers with (even, even) indices are from tiles. Using this logical indexing approach, a ring array table is developed, listing which modules, pairs, and tiles containing rings are identified during the RICH LVL-1 processing.

The RICH LVL-1 ring-finding algorithm starts by looking for a minimum number of photons in each module. The threshold is set to approximately half the expected number of photoelectrons for a RICH ring. The exact threshold will be determined from further simulations of trigger performance, with attention given to avoiding the double-counting of rings. If the number of photons in a module is above the preset value, the module is considered to contain a ring. Those modules which do not contain a ring are then combined into pairs which are then tested for rings using the same threshold as used for the modules. Those pairs not containing a ring are finally combined into tiles and tested for RICH rings. This scheme prevents over-counting of RICH rings when a ring fits completely within a module. To further reduce over-counting of RICH rings, the ring flags for all elements in a unit cell are ORed and the final ring count is incremented once for each unit cell containing at least one ring.

A schematic diagram of the RICH LVL-1 system is shown in Figs. 11.36 and 11.37. Like all other LVL-1 subdetector systems discussed so far, the RICH LVL-1 analysis is pipelined, with processing of all PMT signals, modules, pairs, and tiles done in parallel in the corresponding pipeline steps, as described below. The time required for each step is also shown below in terms of the number of bunch-crossings.

Step 1 - Flash digitization of PMT signals (1 crossing): The signals from the RICH phototubes are digitized with 3 bit FADC's. The gain of the FADC's will be set so that the output is roughly equal to the number of photo-electrons. We expect a maximum of four photo-electrons in a single PMT for a standard ring. This electronics is included in the RICH FEE.

Step 2 - Module summing (5 crossings): The digitized signals from the 25 PMT's in a module are summed in a pipelined summing tree to produce an 8-bit module sum.

Step 3 - Module hit detection (1 crossing): Each module sum is compared to the preset ring threshold. If the module sum is over threshold, the module is marked as having fired and the sum is cleared so that the found ring will not be duplicated in the pair and tile sums. The module sums and comparator outputs are passed on to Step 4.

Step 4 - Pair summing (1 crossing): The module sums are added in pairs to produce 9-bit pair sums. Each module contributes to two horizontal and two vertical pair sums.

Step 5 - Pair hit detection (1 crossing): Each pair sum is compared to the preset ring threshold. If the pair sum is over threshold, the pair is marked as having fired and the sum is cleared so that the found ring will not be duplicated in the tile sums. The pair sums and comparator outputs are passed on to Step 6.

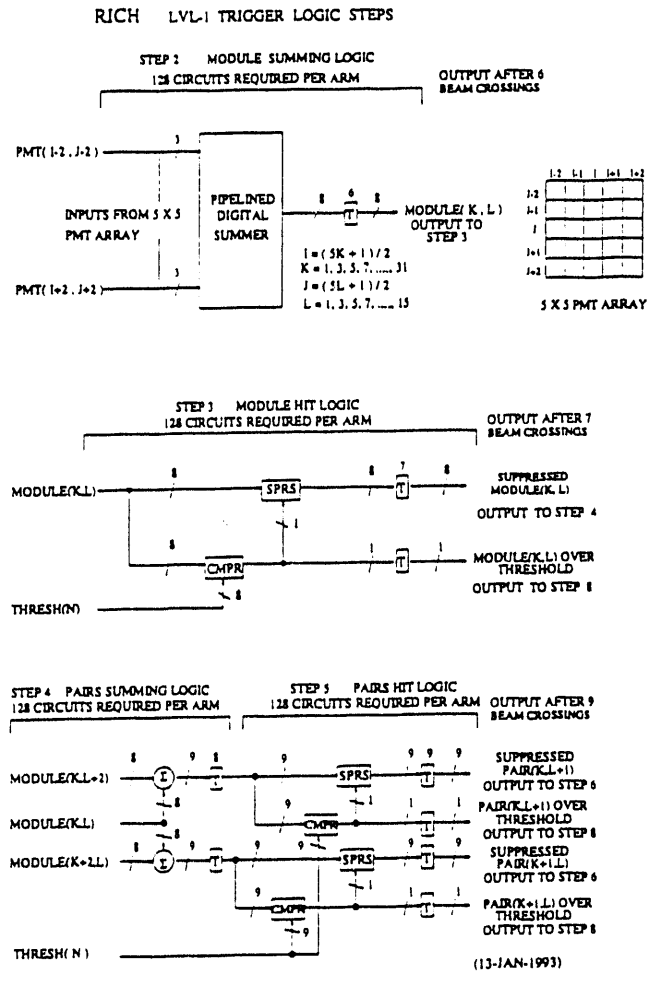

Figure 11.36: Schematic diagram of LVL-1 trigger for RICH (early stages).

Step 6 - Tile Summing (1 crossing): The pair sums are added to produce tile sums. Each tile contains two horizontal and two vertical pairs, some of which may have been cleared in the pair hit detection stage. The goal of this step is to find rings which fall inside of a tile but fail to land well enough inside the pairs or modules which the tile contains so as to fire them. We currently plan to sum all four pairs in a given tile and then divide by 2 before applying the threshold (because in this way the photo-electrons in the tile are counted twice).

Step 7 - Tile hit logic (1 crossing): Tile sums above the ring threshold are marked as containing a ring.

Step 8 - Unit cell hit logic (1 crossing): The hit flags for the elements in each unit cell are ORed to produce a unit cell hit flag. The hit patterns for all unit cells are also loaded into the ring array.

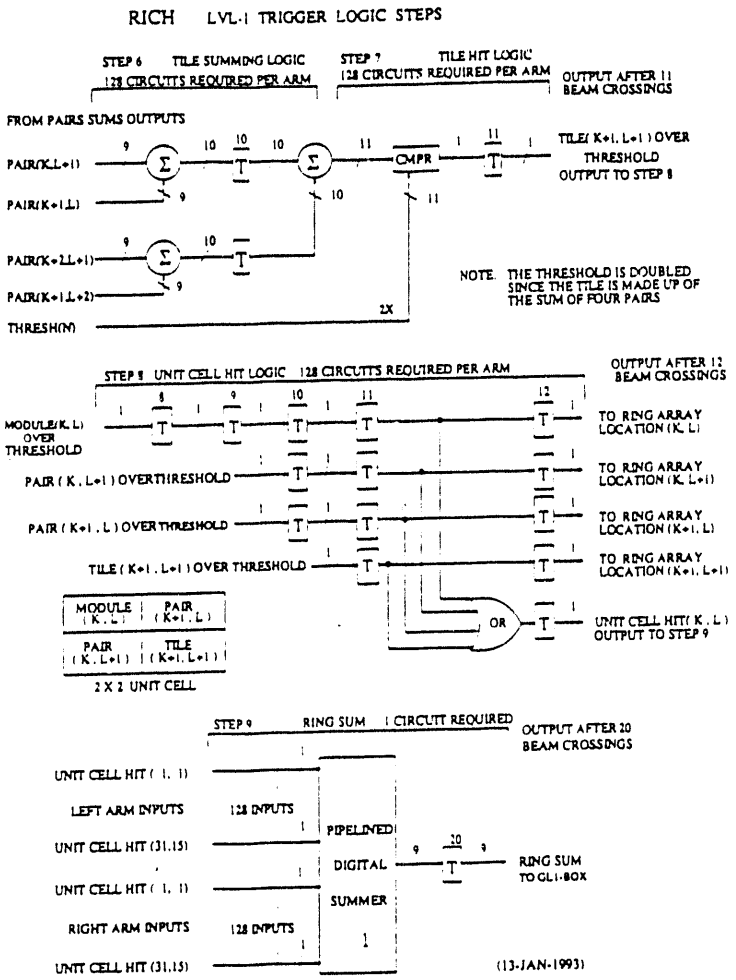

Figure 11.37: Schematic diagram of LVL-1 trigger for RICH (later stages).

Step 9 - Ring sum (8 crossings): The number of unit cells with rings found is counted using a pipelined summing tree to return the number of rings found in the RICH.

The RICH LVL-1 processing produces a ring sum and the 512-element ring array for each RICH arm, which contains for each module, pair, and tile, a flag that indicates whether that element contained a ring. The ring sum, nominally a count of the number of Cherenkov rings seen in the RICH, is sent to GL1. The ring sum and ring array data are added to the event stream and passed to LVL-2.

Time of Flight

The LVL-1 trigger for the high-resolution TOF will be used to trigger on hadronic physics observables in light-ion systems where a LVL-1 trigger is necessary. The trigger is used to

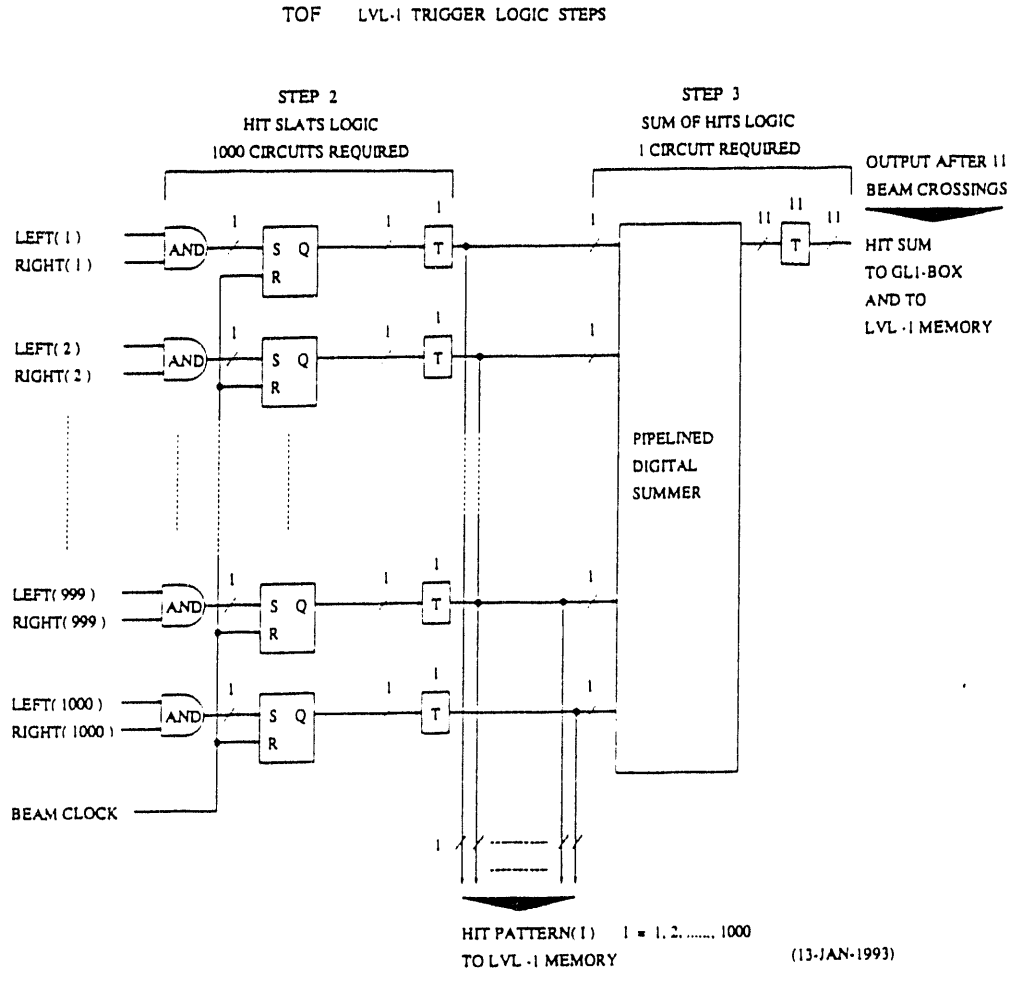

Figure 11.38: Schematic diagram of LVL-1 trigger for TOF.

select events with at least one particle for measurements of single-particle spectra and events with two particles for interferometry and ϕ-meson measurements. The trigger counts the number of hits in the TOF slats and also provides a slat hit-pattern that will be used by the LVL-2 trigger.

A schematic diagram of the LVL-1 trigger system for TOF is shown in Fig. 11.38. The TOF LVL-1 processing pipeline consists of the three steps listed below.

Step 1 - PMT Signal Discrimination (no delay): The TOF PMT outputs are discriminated in the TOF front-end electronics.

Step 2 - Hit Pattern Generation (1 crossing): An AND is taken between the discriminator outputs for the two ends of each slat and these signals are then latched into a pattern register.

Step 3 - Hit Sum (10 crossings): A pipelined summing tree counts the number of TOF hits using the latched pattern word to produce the hit sum.

The hit sum output from the TOF LVL-1 processing is made available to GL1 for use in making a high-resolution TOF trigger. The 1000-bit pattern word indicating which TOF slats were hit is entered into the data stream and presented to the LVL-2 trigger.

Electromagnetic Calorimeter

The EMCal is used at LVL-1 to provide a global trigger on collision centrality and a local trigger for individual electromagnetic (EM) showers whose energy is above the energy deposited by minimum ionizing charged particles. The total energy measured in the EMCal provides an alternative to the charged-particle multiplicities measured in the MVD for event-characterization purposes. The EMCal LVL-1 processing system will also provide the locations of EM showers above specified cuts that can be used to direct the processing in the EMCal LVL-2 trigger. Guidance from LVL-1 is particularly important for the EMCal LVL-2 processing because of the large number of hits in the EMCal from both charged particles and photons.

Currently, there is no charged-particle detector in front of the EMCal with geometry that is well-matched to the EMCal tower arrangement. Thus, the calorimeter cannot currently be used at LVL-1 to distinguish between electron and photon showers. Thus, since the number of photons from π^0 decay overwhelms the number of electrons in all collisions, we treat all energetic EM showers as photons. However, to ensure that a charged-particle detector matched to the EMCal can be used if it is eventually installed, the EMCal LVL-1 trigger includes the logic to perform electron-detection and counting. Energetic electrons will have energies above the minimum-ionizing peaks in the EMCal and will have hits in the associated charged-particle detector. The rejection capability of this electron trigger will be determined by the energy cut used and will be limited by the pion charge-exchange probability and the rate of random coincidences between charged-particles in the front detector and photons in the EMCal.

The EMCal LVL-1 trigger generates four pieces of summary data. "Global Sum", is the total energy measured in the EMCal. The three other sums, "Photon-1 Sum", "Photon-2 Sum", and "Electron Sum" count the numbers of photons and electrons above preset energy cuts. Two photon thresholds (Photon-1 is the higher energy threshold) are used to allow for better trigger rejection in high-multiplicity events for which the tile double-hit probability is much larger. The electron and photon counts are obtained by summing the PMT signals over "tiles" and applying the the energy thresholds and charged-particle matching requirements to the tiles. The tiles are formed from 2×2 arrays of "cells", which in turn are formed from 2×2 blocks of EMCal towers. To reduce the cost of the EMCal LVL-1 trigger system, the cell energies are are obtained by summing analog signals split from the 4 EMCal towers in each cell. These cell analog sums are digitized with 8-bit 10-MHz FADCs and then summed digitally to form the tile sums. The cells are non-overlapping, so there are 7000 cells. The tiles overlap by half their size in both directions, so there are also 7000 tiles. The gain of the cell FADC is set to obtain as large a dynamic range in photon energy as possible, while still

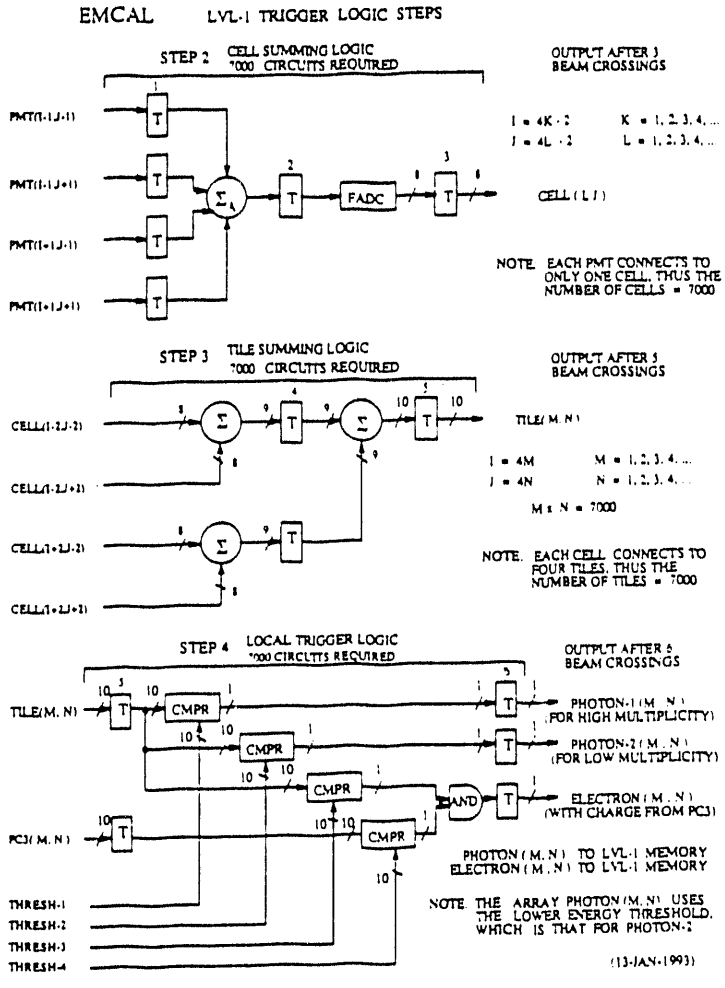

Figure 11.39: Schematic diagram of LVL-1 trigger for EMCal (early stages).

retaining adequate energy resolution for the Global Sum. We currently plan to set the FADC gain such that the upper end of the dynamic range corresponds to 5 GeV. This choice, then, gives a least count equivalent energy of 20 MeV which is well below the expected mean π^0 photon energy of 150 MeV.

A schematic diagram of the LVL-1 processing for the EMCal is shown in Figs. 11.39 and 11.40. The steps in the pipeline are described below.

Step 1 - PMT output (1 crossing): The output is split three ways, to the preamp, the TAC, and the trigger.

Step 2 - Cell Analog Summing and Digitization (2 crossings): Part of the anode current from four PMTs in a 2×2 cell is sent to an analog summing amplifier, whose output is then digitized using an 8-bit 10 MHz FADC.

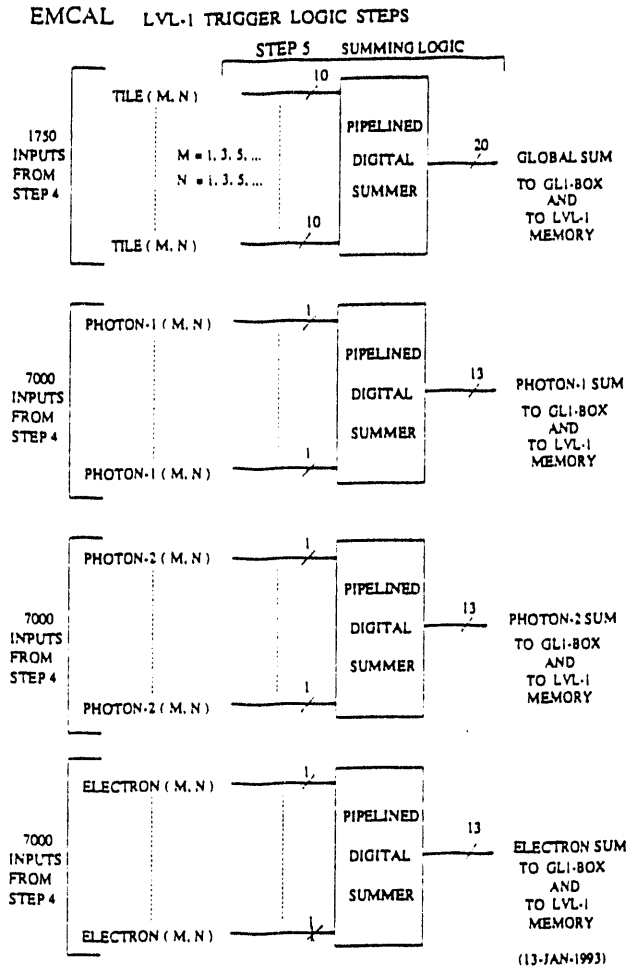

Figure 11.40: Schematic diagram of LVL-1 trigger for EMCal (later stages).

Step 3 - Tile Summing (2 crossings): The cell sums from each tile are added digitally to produce a 10-bit tile sum.

Step 4 - Local trigger logic (1 crossing): The tile sums are compared to the two photon thresholds to produce the two logical outputs "Photon-1" and "Photon-2" for the next stage of processing. The tile sum is also compared to the electron threshold and this comparator output is ANDed with the charged-particle bit associated with the given tile to form the "Electron" logical output. Bits corresponding to the tiles with TRUE Electron and Photon-2 outputs are written into Electron and Photon pattern words.

Step 5 - Global Summing logic (12 crossings): The four sums, Global Sum, Photon-1 Sum, Photon-2 Sum, and Electron Sum are formed in this step. Because the tiles overlap, only one in every four (4) tiles is used to produce the

Global Sum. The other 3 sums are not *energy* sums, but are actually counts of the number of tiles passing the corresponding cuts.

All four of the global sums are provided to the GL1 trigger. The electron and photon pattern words are added to the event stream and provided to LVL-2.

Muon Identifier

The muon detector has one of the more selective LVL-1 triggers. The muon production rate is lower than that for other observables, and the ratio of true pairs to triggered pairs is a factor of 10 larger than that for electrons. Thus, the trigger can provide useful rate reduction at LVL-1. The detection of a pair of muons is relatively straightforward in the acceptance of the muon system so the muon LVL-1 trigger should be easily implemented. and it should place less of a burden on the muon LVL-2 trigger. The muon LVL-1 trigger is designed to find and count tracks penetrating the μID.

As discussed in Chapter 10. the μID consists of a set of three absorber layers, after each of which is a streamer-tube plane with pad readout. The identifier planes are divided into octants with 96 radial pads each. The pads provide the ϕ positions of the tracks at each layer. For LVL-1 triggering purposes, three physical pads are ORed together to produce 32 LVL-1 "pads" per octant, each subtending about 1.5° in azimuth. In the remainder of the discussion below, "pads" will refer to these groups of three physical pads. The muon LVL-1 trigger finds particles that penetrate to the last detector in the μID. Muon "tracks" are required to fire all three planes in a given octant and to have less than a 3° change in ϕ between identifier layers. This condition is applied by requiring the muon tracks to hit the first and third μID layers within ± 2 pads of the track hit on the second μID layer. Muons with momenta greater than 2 GeV/c satisfy these conditions with better than 95% efficiency. There are $32 \times 8 = 256$ candidate roads examined by this scheme.

A schematic diagram of LVL-1 for the μID system is shown in Fig. 11.41. The steps in the μID LL1 pipeline are described below:

Step 1 - Pad Hit Finding (1 crossing): The pad signals are discriminated in the front-end electronics of the μID system (not shown in Fig. 11.41).

Step 2 - Pad Set Logic (1 crossing): A logical OR is formed from the 3 pads in each Pad Set.

Steps 3 and 4 - Track Finding Logic (1 crossing each): Groups of 5 pads, each group offset by one pad, are ORed together in layers 1 and 3 (Step 3). Using the index I for the position of the middle pad in a group, an AND is formed between the Ith pad in layer 2 and the Ith pad groups in layers 1 and 3. This step produces 256 bits, each bit indicating whether or not a candidate track was found.

Step 5 - Muon Counting (8 crossings): The 256 bits produced by Step 4 are tallied to produce a 9-bit muon count.

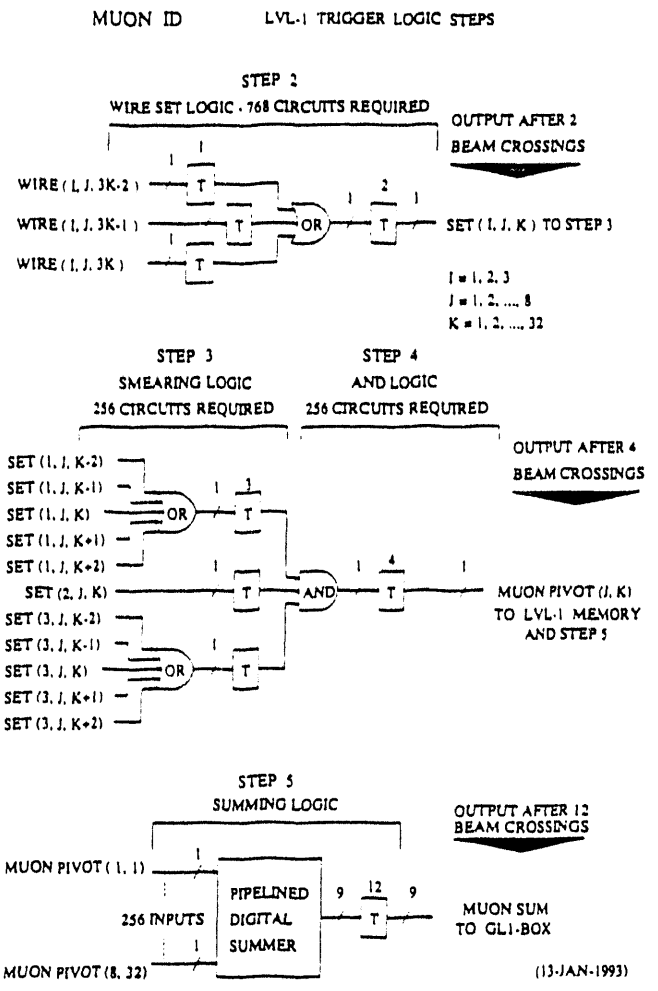

Figure 11.41: Schematic diagram of LVL-1 trigger for Muon-ID

The LVL-1 trigger for the muon system provides two outputs: a "muon count" and the set of pad positions on the second μID layer for the found tracks. The muon count is used in GL1 to make muon-pair triggers and e-μ coincidence triggers. The pad positions on the second μID layer will be used by the muon track finding/fitting algorithm at LVL-2.

Global Level-1 Trigger

The Global LVL-1 (GL1) "Logic Box" makes the actual decision as to whether or not an event is to be digitized. This decision will be made using the LL1 results produced by the various detector subsystems included in the trigger. Because the PHENIX collaboration is interested in studying many different physics observables, the GL1 trigger must be able to apply many different selection criteria in parallel. Because we will want to trigger simultaneously on rare events (massive e^+e^- pairs, $\mu^+\mu^-$ pairs, J/ψ, Υ, high p_T photons, etc.) and minimum bias events, we must have the capability to pre-scale all the various parallel trigger paths. The

GL1 Logic Box must be sufficiently programmable to allow implementation of new selection criteria without significant changes in hardware or cabling, and it must be extendable so that new detector sub-systems can be added without requiring major modifications.

The input data to the GL1 Logic Box in the current LVL-1 design are summarized below.

Status information

Left Status and Right Status - Two 1-bit words indicating whether the Left and Right beam buckets are Full or Empty.

Calibration Status - A 1-bit word indicating whether or not the event is a calibration event.

Transfer FIFO Status - A 1-bit word which indicates whether the transfer FIFO is able or unable to accept events. A value of 1 for this word means impending dead-time, which is a situation in which events already in the LVL-1 pipeline need to be rejected and the pipeline flushed. A value of 0 for this word means able to accept events.

Beam-Beam Status and Timing

Validity Flag - Indicates whether both BB arrays have fired, and if so, whether the vertex position and timing T0 are valid.

Event Flag - Indicates whether at least one of the BB arrays has fired.

Centrality Measurements

Global Sum (E_T) - Total energy in the EMCal.

Total Sum (Multiplicity) - Total number of hits seen in MVD.

Left and Right Sums (Multiplicity) - Multiplicities in left and right halves of MVD (divided at $z = 0$).

Electron Candidates

Ring Sum - Count of Cherenkov ring candidates from the RICH.

Electron Sum - Count of electrons from EMCal (only if front charged-particle detector present).

Photon Candidates

Photon-1 and Photon-2 Sums - Counts of EMCal towers with energy above high (Photon-1) and low (Photon-2) thresholds.

Muon Candidates

Muon Sum - Count of muon candidates.

Hadrons

Hit Sum - Number of hit slats in TOF wall.

All GL1 trigger decisions other than the lowest level interaction trigger will require combining data from different sub-systems. Some of the LVL-1 trigger decisions will only require an AND between a "valid interaction" decision based on the BB data and a threshold on an energy sum or multiplicity. However, some of the observables of interest to the experiment require more sophisticated correlations. For example, we plan to use the Photon-2 sum, which counts photons above a relatively low energy threshold, in low-multiplicity events where the photon showers are well separated and plan to rely more on the Photon-1 sum, which uses a higher threshold, in the higher multiplicity events. In order to implement such a trigger decision, to provide the necessary flexibility in the trigger, and to make the GL1 trigger decision fully programmable, we envision using lookup tables to make the parallel trigger decisions. The lookup scheme allows the trigger to combine data from different subsystems to make a trigger decision that is fully programmable.

The simplest way to implement the lookup scheme would be to use a 2^N address RAM, where N is the number of bits provided to the GL1 "Logic Box", with the output word providing the parallel trigger results. For this scheme to work, the number of bits must be reduced from the 140 bits provided by the detector sub-systems. A scheme to do this is discussed below, but even with this scheme we will have 20-30 bits of data with which to make a LVL-1 decision. To allow for LL1 processing algorithms that are not in our current design and to allow for addition of other detector sub-systems to the LVL-1 trigger, we may not be able to use a single lookup table to make our LVL-1 decisions. If we break the GL1 decision up into stages, we can use smaller lookup tables in the intermediate stages and use a final lookup to produce the final GL1 trigger results. For example, the BB inputs, the accelerator status signals, and the transfer FIFO status signal can be combined to produce a single "valid interaction" bit. Similarly, the MVD provides 3 different multiplicity sums and the EMCal provides an E_T sum for triggering on centrality. The "centrality" decision can be made using these data and a single-bit result can be passed on to later stages of lookup. Ideally, the internal interconnections of the Logic Box would be programmable so that new trigger paths could be implemented by routing a given set of signals to a given lookup table at each intermediate stage.

As discussed in the preceeding paragraph, the number of bits provided to the GL1 Logic Box must be reduced before a final LVL-1 decision can be made. Many of the inputs to the GL1 trigger are in the form of particle counts or energy sums. We will not be interested in the exact values of these inputs but rather in whether or not they fall within a given range of energy or multiplicity. We have designed a device called a Programmable Prescaleable Multilevel Discriminator (PPMD) that takes as input a number and produces a 3-bit word indicating which of 7 programmed thresholds the input number exceeds. This device, then,

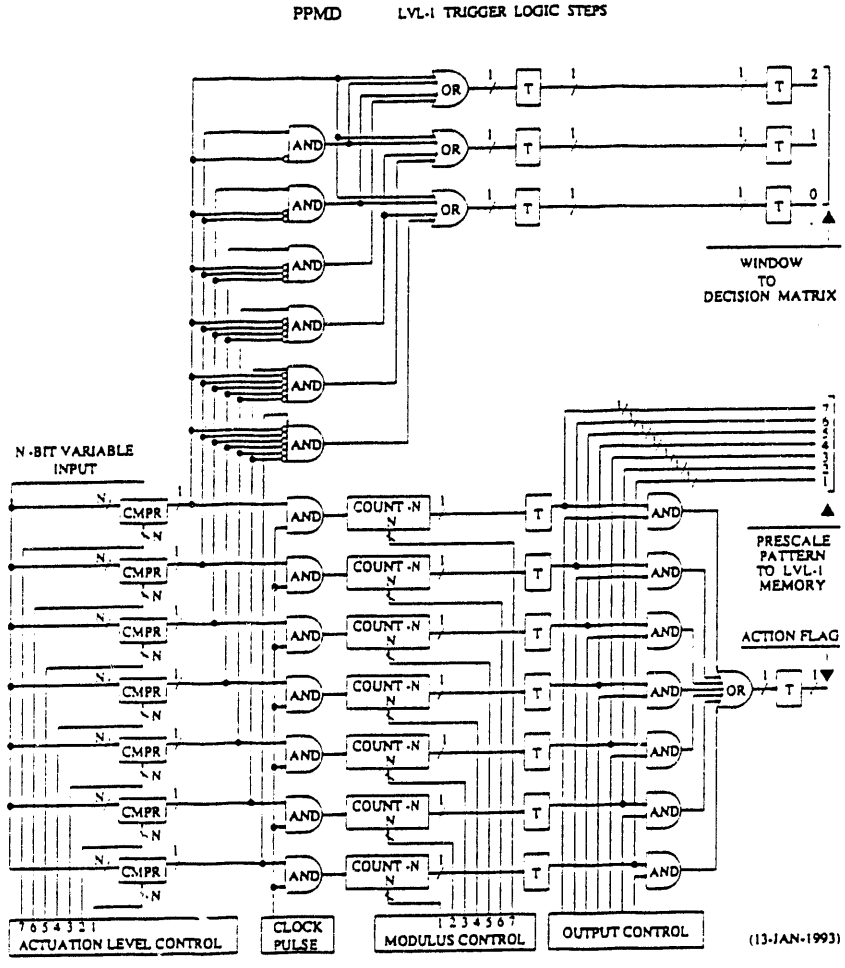

Figure 11.42: Schematic diagram of a PPMD.

reduces the number of bits that must be used in the GL1 lookup tables for for all multiplicities and energy sums. The PPMDs provide pre-scalers for each threshold and produce a single output bit associated with the 3-bit threshold word that can be directly used to produce pre-scaled triggers. For example a PPMD could be used to produce a multiplicity filter. The PPMD could be set to trigger on every event above a high multiplicity (for central collisions), every fourth event above a lower multiplicity (for events of intermediate impact parameters), and so forth, down perhaps to only every hundredth event above a very low multiplicity (for grazing collisions). A schematic diagram for a PPMD is shown in Fig. 11.42.

The GL1 Logic Box will produce a mask of trigger bits, one for each trigger decision. These trigger bits will be passed through a final pre-scale stage and then ORed to produce the final LVL-1 trigger decision.

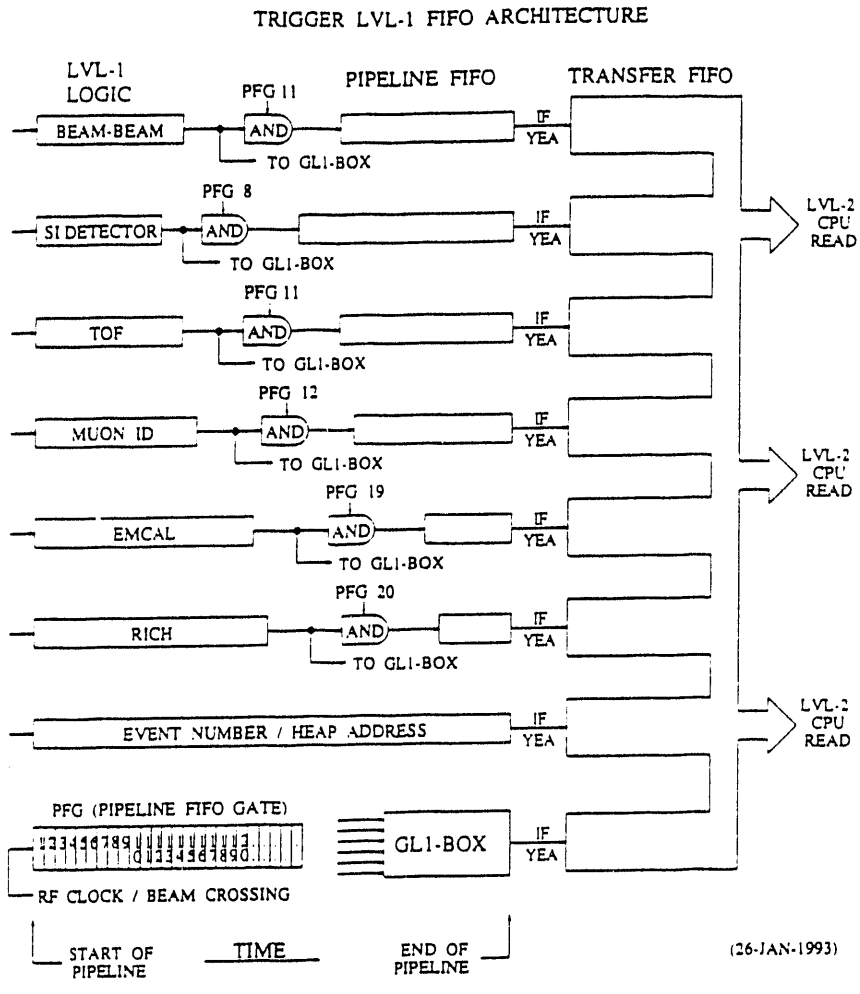

Figure 11.43: Data flow into and schematic diagram of LVL-1 FIFO.

LVL-1 FIFO Architecture

The FIFO (First In, First Out) memory architecture proposed for use by the LVL-1 system provides solutions to several problems. These include problems of timing synchronization between different detector subsystems resulting from differences in the number of stages necessary to perform LVL-1 logic in a pipelined fashion, and access and addressing requirements imposed as a part of the transition from the hardware pipeline architecture of LVL-1 and the "event pipeline" structure of the following LVL-2 and DAQ stages. A schematic diagram of the LVL-1 FIFO architecture and the dataflow into it is shown in Fig. 11.43.

Figure 11.43 shows that the FIFO architecture for LVL-1 actually employs two FIFO memories. The first of these, denoted on the figure as "pipeline FIFO" retains all information generated by the LVL-1 system prior to any decision regarding the disposition of the data. Events enter and leave this FIFO at the beam crossing rate. The second, denoted as "transfer FIFO," receives all LVL-1 data for those events "accepted" by the logic box as requiring

further attention. Events enter this memory at pseudo-random times, but they retain their sequential order. They leave the memory when LVL-2 indicates that all required information for a given event has been absorbed by LVL-2.

Each of the different LVL-1 subsystems providing information to the pipeline FIFO is described elsewhere in this document. Pertinent to this discussion are the following points:

1. The algorithm processing time (as measured in number of beam crossings) may be different for each subsystem trigger.

2. The amount of storage required for each subsystem trigger varies from a few bits generated by the logic box to several thousand words generated by the EMCal trigger subsystem.

3. At the end of the LVL-1 pipeline, a decision must be made to accept or reject the event corresponding to that particular pipeline time slot.

4. The decisions implied by item (3) above must be made for each beam crossing at the beam crossing rate.

As proposed for LVL-1, one may think of the first event entering the pipeline hardware. As discussed elsewhere, the subsystem requiring the least processing time is the MVD. The data from that subsystem requires only a few beam crossings to process, at which time the data is passed on to a portion of the pipeline FIFO memory system and immediately falls through to the output pins where it will remain until it is strobed with a "read" command.

The latest data generated by LVL-1 comes from the GL1 box, which actually makes the "accept/reject" decision. Here certain information associated with the decision making process is passed on to the pipeline FIFO within only a few beam crossings of the "accept/reject" signal.

The remaining subsystems all provide information to the FIFO memory at times intermediate between these extremes. The important point is that if the first "read" signal transferring information out of the FIFO is delayed until all subsystems have submitted their first inputs, then that event from each subsystem "falls" through the FIFO to arrive at its output pins time-aligned with all the other subsystems. Since further inputs occur at the beam crossing rate, all further data retains its appropriate time alignment simply because all events are strictly sequential in time.

The necessary timing control hardware responsible for starting and stopping the pipeline FIFO is depicted in the lower left corner of Fig. 11.43, where it is designated "PFG" (pipeline FIFO gate). This unit consists a of series of delay flip-flops driven by an SR flip-flop. Each delay flip-flop provides an output to a two-input AND circuit whose second input is driven by the BC clock stream. The outputs from these AND's become the clock streams for each level of the pipeline logic.

In its "off" state, the SR flip-flop injects zeros into the delay chain, so that all the clock streams for the pipeline stages are turned off. When the control flip-flop is set "on," that change ripples through the PFG, turning on each each stage of the pipeline clock stream in the appropriate order so that a "wave" of operation propagates through the pipeline hardware.

Starting the pipeline operation in this fashion is sufficient to ensure that all elements of the "first" event reach the pipeline FIFO appropriately timed. Likewise, the same logic insures that when the pipeline is switched off, the various pipeline stages continue to function in such a manner that the pipeline FIFO is emptied of all information in accordance with appropriate decisions by the logic box.

Under static operating conditions, the elements of the pipeline FIFO exhibit "depths" appropriate to the particular subsystem data stream with which it is associated. The "deepest" FIFO would be those elements accepting information from the MVD, while the FIFO accepting information from the logic box would never contain more than a few pieces of information.

All events accepted by the logic box are passed on to the transfer FIFO. This memory serves primarily as a data storage buffer for LVL-2. However it also marks the point at which the trigger and data processing mechanism changes from a synchronous pipeline organization to an "event" pipeline organization. As a part of this transition, the very long data word which is the transfer FIFO output, is subdivided in a manner appropriate to the addressing scheme required by LVL-2, so that information from each subsystem for a given event may be readily located within some consistent format. A given event, as represented by the entire data word at the output of transfer FIFO, would be retained until such time as LVL-2 decides that it is no longer needed (i.e., to be read out or discarded), then a read command to the transfer FIFO would transfer the next word to the output pins for consideration.

11.3.4 Level-2 Trigger

Algorithms

To develop the requirements and specifications of the LVL-2 triggering system, knowledge of the algorithms intended for use in this system is necessary. Table 11.8 lists the rates for production of various physics observables which experience from ongoing AGS and SPS heavy-ion experiments suggests may be of interest.

In this calculation, the rates for hadronic observables were calculated using the limited solid-angle high-resolution time-of-flight wall only. The event rate has been obtained by limiting the tape-writing rate to our stated limit of 20 Mbyte/sec, assuming no LVL-1 reduction beyond what is necessary to bring the raw event rate down to 31 kHz, and no LVL-2 enhancement of the given observables. The table makes it clear that the rates for most of the hadronic observables are sufficient to provide necessary statistics in a matter of days for all systems except p + A collisions. For example, even in central O + O collisions with no LVL-1 or LVL-2 selection, we would record 5000 K^+K^+ pairs per day. To do a straightforward two-dimensional HBT analysis we would want of order 50K pairs, which could be accumulated in 10 days of running. Clearly we would like to do better than this since we will want to run other physics in parallel, but the raw untriggered rates are within a factor of 10 of what we might reasonably expect. On the other hand, the rates for true electron pairs and muon pairs are down by a factor of 100. Clearly, the most important function of the LVL-2 trigger will be to enhance our ability to record these rare events on tape relative to the more common events.

DATE
FILMED
1/27/94
END